Post–orogenic shoshonitic magmas of the Yzerfontein pluton, South Africa: the 'smoking gun' of mantle melting and crustal growth during Cape granite genesis?

J. D. Clemens, I. S. Buick, D. Frei, C. Lana and A. Villaros

Abstract

The post-orogenic Yzerfontein pluton, in the Saldania Belt of South Africa was constructed through numerous injections of shoshonitic magmas. Most magma compositions are adequately modelled as products of fractionation, but the monzogranites and syenogranites may have a separate origin. A separate high-Mg mafic series has a less radiogenic mantle source. Fine-grained magmatic enclaves in the intermediate shoshonitic rocks are autoliths. The pluton was emplaced between 533 ± 3 and 537 ± 3 Ma (LASF-ICP-MS U–Pb zircon), essentially synchronously with many granitic magmas of the Cape Granite Suite (CGS). Yzerfontein may represent a high-level expression of the mantle heat source that initiated partial melting of the local crust and produced the CGS granitic magmas, late in the Saldanian Orogeny. However, magma mixing is not evident at emplacement level and there are no magmatic kinships with the I-type granitic rocks of the CGS. The mantle wedge is inferred to have been enriched during subduction along the active continental margin. In the late- to post-orogenic phase, the enriched mantle partially melted to produce heterogeneous magma batches, exemplified by those that formed the Yzerfontein pluton, which was further hybridized through minor assimilation of crustal materials. Like Yzerfontein, the small volumes of mafic rocks associated with many batholiths, worldwide, are probably also lowvolume, high-level expressions of crustal growth through the emplacement of major amounts of mafic magma into the deep crust.

Introduction and regional context

Granitic magmas are most commonly dominated by crustal components, so partial melting of crustal rocks is essential to their formation (e.g., White and Chappell 1977; Clemens 2006, 2012; Glazner et al. 2015). It has long been appreciated that, in many tectonic settings, to accomplish significant degrees of crustal melting requires the introduction of extra-crustal heat, most likely in the form of under- or intra-plated mantle-derived magmas (e.g., Clemens 1990; Thompson 1990; Vielzeuf et al. 1990).

It is rare to find terranes in which voluminous granitic rocks are accompanied by significant volumes of mafic rocks that could represent the heat source for crustal melting, the 'smoking gun' as it were. This is thought to be the case because regions in which the deep crust is 'fertile' (i.e., capable of extensive partial melting at realisable

temperatures) buffer the temperature of high-grade metamorphism through the heat capacities of the rocks and the latent heat of melting (Vielzeuf et al. 1990). Thus, these mantle-derived magmas represent significant crustal additions or continental crustal growth (Clemens 1990; Rudnick 1990) but are commonly fully crystallised and remain in the deep crust (e.g., Pin 1990), with little or no representation at shallow crustal levels where the granitic magmas are commonly emplaced. Exceptions may be the tiny volumes represented by the highly hybridised igneous microgranular enclaves that are common in many granitic rocks (e.g., Clemens et al. 2016, Clemens et al. 2017; Dorais et al. 1990; Elburg and Nicholls 1995; Vernon 1984). Other possible examples include some calc-alkaline to tholeiitic complexes in which larger volumes of mafic to intermediate magmas co-existed with the granitic magmas, commonly in mingling relationships (e.g., Pitcher 1997; Słaby and Martin 2008). However, as stated earlier, in many cases there is little geological sign of the necessarily large mafic heat source (e.g., the very voluminous Late Devonian felsic magmatic province of Central Victoria in Australia; Clemens and Phillips 2014; Clemens et al. 2016).

Nevertheless, other than hybridised enclaves, some mafic magmatism is generally contemporaneous with the granitic magmatism. For example, in the case of Central Victoria the main manifestation of this is the mafic to ultramafic Woods Point Dyke Swarm (Bierlein et al. 2001). Here, we describe the mafic Yzerfontein pluton, from the Neoproterozoic-Cambrian Saldania Belt of southwestern South Africa, which is spatially associated with the Cape Granite Suite (CGS), and we explore the possibility that this represents a high-level expression of the mantle magmatism that was responsible for lower-crustal partial melting and the genesis of the felsic magmas of the CGS. Although the Yzerfontein pluton has been the subject of several small geochemical (Maske 1957; Jordaan 1990; Jordaan et al. 1995) and a single geochronological study (Jordaan et al. 1995), its emplacement age is poorly constrained, its geochemical and isotopic affinities, if any, with other intrusive rocks in the CGS are poorly understood, and the petrogenesis of the pluton has not been placed in the context of recently developed models for the tectonic setting of the Saldania Belt. In this contribution, we demonstrate that the Yzerfontein pluton is indeed contemporaneous with the early phases of the felsic magmatism here, and that the magmas involved, though they have some crustal characteristics, must ultimately have been derived from enriched-mantle sources. We suggest that such minor occurrences of small-volume mafic to intermediate igneous rocks that accompany voluminous granitic plutons are indeed the 'smoking gun' of mantle heat that served to partially melt the crust and form the granitic magmas.

The Yzerfontein pluton and granites of the CGS intruded low-grade metasedimentary rocks of the Saldania Belt, which developed in the overlying plate above a southeast-dipping Neoproterozoic to Cambrian subduction zone, west of the Kalahari Craton, that consumed the Adamastor ocean (Goscombe et al. 2003; Goscombe and Gray 2008; Kisters and Belcher 2017). Based on U–Pb zircon data from Scheepers (1995), Da Silva et al. (2000), Scheepers and Armstrong (2002), Chemale et al. (2011) and Villaros et al. (2012) the main plutonic phase of the CGS in the Western Cape sector of the Saldania Belt is comprised of dominant S-type (550–530 Ma), smaller volumes of I-type (540–530 Ma) plutons, and a few small A-type plutons (525–510 Ma), with an inferred progression from S- to I- to A-type magmatism. The granitic plutons have traditionally been regarded

as post-tectonic (e.g., Scheepers 1995; Scheepers and Schoch 2006). Indeed, they are generally unfoliated and cut across both regional structures and local fabrics in the wall rocks. However, as pointed out by Kisters and Belcher (2017), at this stage in the development of the orogen, regional transpression was partitioned strongly into major shear zones (Kisters et al. 2002) and the granites that are intruded into these active zones have strong syn-magmatic fabrics. Hence, the CGS should be regarded as mainly latetectonic rather than wholly post-tectonic. Note that the degree of crustal thickening at this time was small, since we have thin, subaerially deposited rhyolite ignimbrite sequences (of CGS age) preserved within the Western Cape sector of the Belt (e.g., Scheepers and Nortjé 2000; Clemens and Stevens 2016). This indicates small degrees of post-orogenic uplift and, therefore, of original thickening.

In addition to the CGS granitic plutons, there are several potassic, mafic to intermediate, intrusive bodies (the Yzerfontein, Mud River and Boterberg plutons) that are spatially and temporally associated with the felsic rocks on the south-western side of the Colenso Fault (Fig. 1), though these were generally held to be significantly younger than the S- and I-type granitic rocks of the CGS (Jordaan et al. 1995). Probably the largest of this group of mafic bodies is the Yzerfontein pluton, located near the coastal village of Yzerfontein, south of Langebaan (Fig. 1). Jordaan et al. (1995) recognised the composite character of the Yzerfontein pluton, noting the existence of several intrusive phases (e.g., Fig. 2). The basement rocks here are members of the greenschist facies, mainly metasedimentary, Neoproterozoic Malmesbury Group, although the exact geological context of the coastal exposures is obscured by inland Cenozoic cover, including sand dunes. Most outcrops of the Yzerfontein pluton occur along the coastline, on a few offshore islands and on a ridge about 1 km inland (Jordaan et al. 1995). A magnetic anomaly map, mentioned but not referenced by Jordaan et al., is interpreted to suggest that the intrusion is only slightly larger than the total extent of the main exposure. Frimmel et al. (2013) dated the deposition of the Malmesbury Group as up to 557 and 552 Ma, and assigned to them a back-arc tectonic setting. This maximum depositional age is consistent with the c. 555 Ma crystallisation age for a felsic tuff in the Malmesbury Group (Kisters et al. 2015).
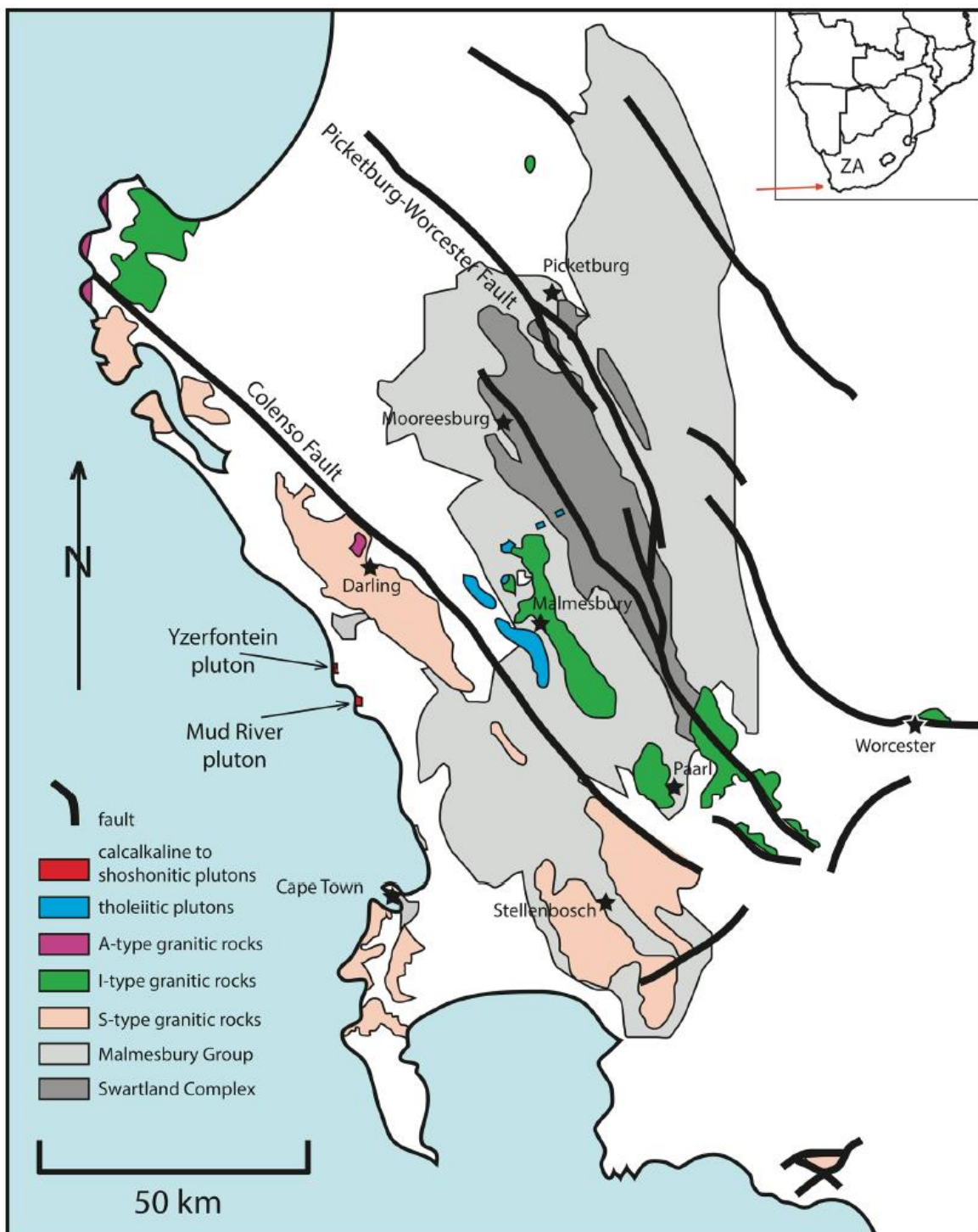
Fig. 1 Sketch map showing the geological context of the Yzerfontein pluton and associated rocks in the western Saldania Belt, South Africa. The approximate areas of exposure of the Late Proterozoic Swartland complex and Malmesbury Group are adapted from Fig. 3 of Kisters and Belcher (2017). The *inset* shows southern Africa, with South Africa labelled ZA and the location of the main map indicated by a *red arrow*

Hartnady et al. (1974) and Belcher and Kisters (2003) described the Malmesbury Group as a complex accretionary tectonic mélange. The most recent interpretation (Kisters and Belcher 2017) is that the Malmesbury Group represents a strongly deformed fore-arc basin that overlies an accretionary prism, the lower parts of which form the Swartland complex, formerly thought of as lower Malmesbury Group. The Swartland complex encompasses large parts of the Swartland Subgroup (e.g., SACS 1980; Gresse et al. 2006). Figure 1 shows the inferred areas of exposure of these Late Proterozoic rocks.

4

Fig. 2 An outcrop of rocks from to the main (shoshonitic) series (see text) of the Yzerfontein pluton. Note the general absence of gradational contacts between the three different rock types and the preponderance of intrusive and medium-scale mechanical mingling features. For scale, the shaft of the hammer is 60 cm long

Within analytical uncertainty, the youngest concordant detrital zircon ages from the Malmesbury Group/Swartland complex overlap with the oldest emplacement ages for the S-type granites of the CGS (Scheepers and Armstrong 2002), which led to the suggestion that the Malmesbury Group, at depth, formed the protolith for the granitic magmas (Harris and Vogeli 2010; Villaros 2010; Villaros et al. 2012). The Yzerfontein mafic to intermediate rocks are potassic in character and purportedly high-K calc-alkaline (Scheepers 1995; Jordaan et al. 1995), though actually shoshonitic (see later). Along with the A-type granitic rocks of the CGS, they have been grouped as part of a late phase of Cambrian magmatism in the region (phase III, emplaced between 530 and 500 Ma; Da Silva et al. 2000; Chemale et al. 2011) and are supposed to be anorogenic in setting (Scheepers 1995; Jordaan et al. 1995).

Some details of the chemistry and petrology of the Yzerfontein pluton have previously been studied in the MSc thesis of Jordaan (1990) and published as part of Jordaan et al. (1995). These authors interpreted the existing age and chemical data to indicate that the Yzerfontein and Mud River plutons form the mafic portion of the high-K, calcal-kaline, CGS, I-type granite association. There are also field and some analytical data from Maske (1957). The additional whole-rock chemical data presented here represent samples collected, mainly from the monzonitic portion of the pluton, as part of the BSc honours project of Hugo (2011). Electronic Appendix EA1 shows the locations and identities of all

samples taken for the present work, as well as for those from Maske (1957) and Jordaan et al. (1995). Coordinates are exact for some and closely approximate for others from the present sample set, approximate for all those of Maske (1957), but more precise for those from Jordaan et al. (1995). These were augmented subsequently with our new Sr and Nd whole-rock isotope analyses and zircon U–Pb geochronological and Hf isotope work. As detailed in Electronic Appendix EA2 (analytical methods), the new whole-rock isotope analyses were carried out at AEON Labs, University of Cape Town, the U–Pb isotope work in the Central Analytical Facility of the University of Stellenbosch and the zircon Hf isotope work in the Department of Geology, Federal University of Ouro Preto (Minas Gerais, Brazil). Some other Sr and Nd isotope data were sourced from Frimmel et al. (2013). Additional Sr and Nd isotope data for Malmesbury Group metasediments and for plutons of the CGS were obtained from the School of Earth and Environmental Sciences, the University of Adelaide, Australia. All radiogenic isotope data have been recalculated to a reference age of 535 Ma, our new crystallisation age for the Yzerfontein pluton (see below).

The present work collates the chemical (Electronic Appendix EA3) and petrological data for the Yzerfontein pluton, to assess its magmatic affinities (especially its relationship with the I-type granitic rocks of the CGS) and to draw some inferences on the genesis of the magmas. The nature of the probable mantle end member and the roles of various petrogenetic processes in shaping the present rock compositions are examined. Electronic Appendix EA3 also contains some data on the chemistry of the volumetrically major metasedimentary types from the Malmesbury Group and Swartland complex. We have used zircon U–Pb geo-chronology to obtain new U–Pb age data for the Yzerfontein rocks and thus locate this mafic magmatism better within the context of the overall CGS magmatic cycle.

Local geological context and previous work on the Yzerfontein pluton
Mafic rocks
The pluton has long been known to be composite, with some parts displaying prominent or more subtle layering on scales of decimetres to metres. According to Jordaan et al. (1995) the rocks of the pluton all belong to the high-K calc-alkaline series, and have compositions that vary from olivine gabbros to quartz monzonites, with monzonitic rocks being dominant. Using the TAS classification scheme of Le Bas and Streckeisen (1991) and Le Maitre et al. (2002), with modifications for plutonic rocks by Middlemost (1994), excluding both dyke rocks and enclaves and assuming that the analysed samples are representative of the pluton's contents, the most abundant rocks are quartz monzonites. The next most abundant are monzonites, quartz monzodiorites and quartz diorites. There are small volumes of syenites and gabbros and very small volumes of monzodiorites and diorites. The more gabbroic rocks, in the northernmost part of the pluton, show more prominent layering than the monzonitic to dioritic rocks that form the bulk of the pluton (Maske 1957; Jordaan et al. 1995). This layering is defined by variations in feldspar–pyroxene ratios. According to Maske (1957), the structures in the monzonitic rocks are discordant with those in the presumably slightly earlier-emplaced gabbroic rocks. Maske therefore ruled out in situ differentiation of the gabbroic magmas as the origin of the monzonitic magmas.

6

Jordaan et al. ([1995](#)) dated the pluton by ID-TIMS U–Pb analysis of a composite zircon separate from five monzonitic to monzodioritic rocks. The U–Pb isotope data were discordant, yielding an upper intercept age of 519 ± 7 Ma, and a lower intercept consistent with recent Pb loss. In view of the discordance of these data, Jordaan et al. interpreted the upper intercept to represent a minimum estimate for the emplacement age. The 519 Ma date suggested that Yzerfontein is considerably younger than the main I- and S-type felsic plutons of the CGS but roughly coeval with the later A-type plutons as well as the existing crystallisation age for the S-type ignimbrites in the same general area. Jordaan et al. also published some Sr isotope data and calculated initial $^{87}Sr/^{86}Sr$ based on their 519 Ma age.

Xenoliths of metasediments and granitic rocks appear to be completely absent from the Yzerfontein pluton. However, in some places, the monzonitic rocks enclose numerous, rounded, cm- to dm-sized, fine-grained, melanocratic magmatic enclaves. Our petrographic and chemical investigations show that these are quartz microdiorites, micromonzodiorites and quartz micromonzonites, in about equal proportions, and we interpret them as autoliths—quenched fractions of the magmas of the main pluton. Their commonly aphyric or sparsely porphyritic character further shows that the shoshonitic rocks crystallised from essentially liquid magmas and that the rudimentary layering in them must have formed by crystal segregation at emplacement level, following some cooling and crystallisation.

Jordaan et al. ([1995](#), p. 61) also note small "patches of mafic material in gradational contact with monzonite". These features suggest the possibility of roles for processes such as magma mixing and mingling in the chemical evolution of the Yzerfontein magmas. However, as shown in Fig. [2](#), the field relations suggest that, at emplacement level, interactions between magmas were close to purely mechanical, with intrusive contacts and mingling textures dominating. If mixing played a significant role, it must have done so at greater depth. We investigate this question further using analyses of both host rocks and enclaves.

Felsic rocks
Most of the analysed felsic rocks occur as late dykes that cut the monzonitic part of the pluton. Chemically they are mainly quartz syenites, though there are also syenites, monzogranites, syenogranites and syenogranitic pegmatites. Jordaan et al. ([1995](#)) note the presence of two 'large' bodies of 'aplite', net-veining part of the monzonitic section of the pluton as well as several smaller (decimetric), planar 'aplitic' dykes cutting the monzonitic rocks. Although we cannot be certain about all these, our field and thin-section observations suggest that many of these dykes are sugary-textured, hypabyssal quartz microsyenites rather than aplites. Some of the true syenogranitic aplites contain tourmaline, which is not found in the more syenitic dykes.

Alteration zones
Especially in the monzonitic part of the pluton, there are numerous hydrothermal alteration zones in veins, along joint planes and in irregular patches. These are stained with hematite and contain combinations of sericite, chlorite, epidote, pyrite, chalcopyrite, calcite and cryptocrystalline silica. In rocks affected by this alteration, the

mafic minerals are chloritised and the plagioclase feldspar is at least partially replaced by sericitic white mica. Our own sampling strictly avoided proximity to these alteration zones. Thus, in thin section, the rocks show typical igneous textures and little or no signs of this late hydrothermal activity (Fig. 3). We, therefore, infer that our analyses reflect compositions close to the original igneous chemistry. The extent of the alteration appears not to be as pervasive as has commonly been mentioned in previous studies, except in the gabbroic section of the pluton. However, we cannot be completely certain of the state of previously analysed rocks.

Petrographic characteristics of newly sampled Yzerfontein rocks

Samples from the present work are numbered H1 to H26 and most have corresponding thin sections. In the composite descriptions below, we use rock names based on the modal mineralogy of each type, allowing us to group rocks with textural and mineralogical similarities. Samples are further grouped according to their field occurrence, as host plutonic rocks, enclaves in those hosts or dykes that intrude the pluton. As noted by previous workers, the monzonitic part of the pluton is highly variable in both its textures and mineralogy.
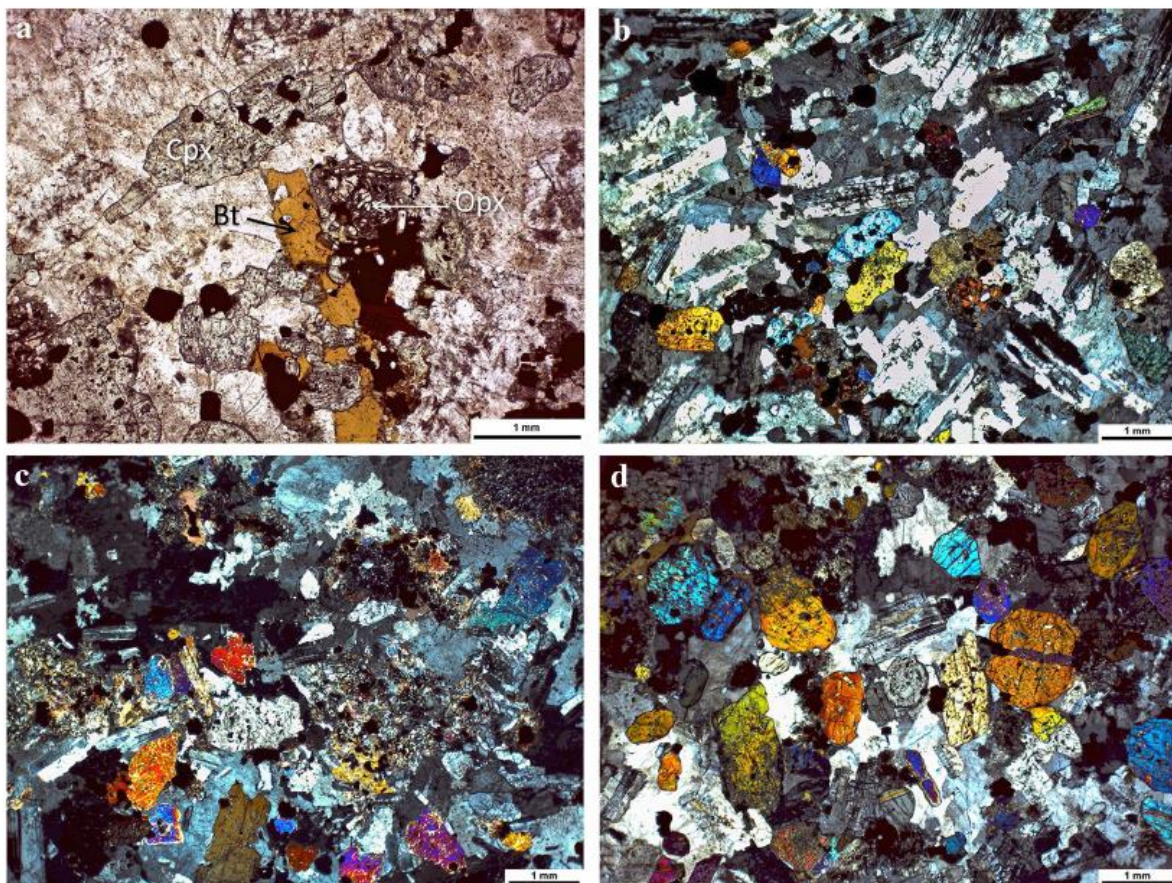

Fig. 3 Photomicrographs of the textures and mineralogy of samples from the Yzerfontein pluton. **a** biotite two-pyroxene monzonite H19 ppl, **b** biotite two-pyroxene monzonite H19 + pol, **c** biotite clinopyroxene hornblende monzonite H9 + pol, **d** biotite hornblende clinopyroxene quartz monzonite H8 + pol

Cumulate hornblendite from the layered (high‑Mg) series (822B)

This rock consists mainly of equant, subhedral crystals of green–brown hornblende with lesser, subhedral, intercumulus plagioclase. Accessory phases include large, euhedral

8

apatite crystals, abundant magnetite and rare anhedral and interstitial reddish-brown biotite and titanite. Some hornblende crystals show near-solidus recrystallisation to fine felted aggregates of actinolitic amphibole. There is also minor, secondary calcite.

Plutonic rocks in the monzonitic part of the pluton
Biotite–hornblende–clinopyroxene quartz monzonites (H8, H15, H17, H21)
These rocks (exemplified by sample H8 in Fig. 3d) have a typical monzonitic fabric, and vary in grainsize from coarse to medium. Large, but variably abundant, anhedral, poikilitic microcline microperthite crystals enclose most of the other mineral grains. The clinopyroxene is subhedral, rounded and prismatic, locally with overgrowths of pale-green clinoamphibole. The prismatic hornblende is generally dull green in colour and the plagioclase forms subhedral to euhedral tablets with complex twinning and normal compositional zoning. The ratio of hornblende to clinopyroxene is quite variable. The biotite, which also varies in proportion, is orange–brown in colour and mainly anhedral. Quartz is relatively scarce and forms interstitial anhedra. Magnetite octahedra and abundant prisms of apatite (some relatively large) are the main accessories, and rare allanite occurs in some samples. In some rocks, magnetite forms clumps of very small grains associated with fine, fibrous hornblende. These may be pseudomorphs after orthopyroxene. Some samples also contain patches of microgranophyre. When present, the secondary phases are small grains of epidote, some fibrous green chlorite, rare green biotite and occasional green chlorite pseudomorphing primary orange–brown biotite.

Clinopyroxene–biotite–hornblende leucomicromonzonite (H6)
In this rock, small, euhedral tablets of plagioclase are set in a fine granular matrix of quartz and K-feldspar, with anhedral hornblende, magnetite and a few shreds of biotite. The scarce clinopyroxene forms euhedral microphenocrysts rimmed by hornblende.

Hornblende–clinopyroxene quartz micromonzonite (H7)
This rock hosts enclaves of micromonzodiorite (e.g., sample H2, described below). Large euhedral crystals of brown–green to blue–green hornblende and colourless clinopyroxene, together with plagioclase laths form the main fabric of the rock. Microperthitic K-feldspar and granular quartz fill the interstices. There is also some late-crystallised, anhedral hornblende. Accessories include magnetite octahedra, apatite prisms and scarce zircons.

Biotite–clinopyroxene–hornblende monzonite (H9)
Abundant subhedral clinopyroxene, anhedral biotite and minor hornblende are poikilitically enclosed by large anhedral microcline microperthite crystals that are simply twinned and show some evidence of marginal recrystallisation (fine polycrystalline growths with lobate grain boundaries). Intergrowths of pale greenish clinoamphibole and magnetite pseudomorph a primary mafic mineral, possibly orthopyroxene. The accessories include magnetite octahedra, shapeless to platy ilmenite and some apatite. Clinopyroxene crystals show minor degrees of replacement by biotite along their grain edges and cleavage planes. Minor secondary phases include epidote and chlorite. Figure 3c illustrates the texture.

Biotite–two‑pyroxene monzonite (H19)

This coarse-grained rock contains subhedral crystals of clinopyroxene, biotite, embayed orthopyroxene and plagioclase tablets all set in large, poikilitic anhedra of microcline microperthite. There are some patches of microgranophyre, relatively large accessory apatite prisms and the usual magnetite octahedra. Figures 3a, b illustrate the texture.

Clinopyroxene–hornblende monzonite (H20)

Unlike most of the other monzonites and quartz monzonites, the K-feldspar in this very coarse-grained rock is not poikilitic but interstitial. The other phases present include large plagioclase tablets, green, subhedral hornblende (some of which is also present as interstitial anhedra), and minor clinopyroxene subhedra with reaction rims of hornblende. Accessories are magnetite and abundant apatite prisms.

Hornblende–pyroxene quartz monzodiorite (H3, H17, H25, H26)

These medium- to coarse-grained rocks have monzonitic textures with large and abundant, subhedral, multiply twinned clinopyroxene, lesser yellow–green hornblende prisms (very scarce in H25 and H26), minor embayed orthopyroxene prisms (absent in H25 and H26), euhedral, unzoned plagioclase tablets or laths, rare interstitial biotite (absent in H3 and H17 and more abundant in H26), and accessory magnetite and abundant apatite prisms, all set in large, poikilitic K-feldspar crystals, with very rare interstitial quartz and even scarcer titanite. In some rocks, there is minor replacement of the hornblende by felted actinolitic amphibole. Some examples are strongly ophitic in texture; the large (2 cm), irregularly distributed clinopyroxene oikocrysts enclose small plagioclase laths. These clinopyroxenes give the rock a blotchy appearance in hand specimen. In some cases, the coarse-grained monzodiorites have decimetric layering defined by variations in pyroxene abundance. When present, secondary minerals include chlorite (mainly after biotite) and epidote granules.

Enclaves in the main plutonic rocks

Hornblende–biotite quartz micromonzonites (H4, H5, H18)

These fine-grained, aphyric rocks contain biotite, horn-blende, plagioclase and magnetite set in poikilitic K-feldspar crystals in a micromonzonitic texture. The quartz is anhedral and interstitial, and varies in abundance. The biotite is locally replaced by green chlorite and secondary epidote can also be present.

Biotite–two‑pyroxene micromonzonite (H24)

This rock contains microphenocrysts of subhedral clinopyroxene and plagioclase microglomerocrysts set in a ground-mass of plagioclase laths, stubby clinopyroxene euhedra, rare subhedral orthopyroxene, anhedral and poikilitic reddish-brown biotite (with inclusions of plagioclase and accessory minerals) and a little interstitial K-feldspar. The microphenocrysts form about 10% of the rock. Accessory minerals are abundant tiny apatite needles and magnetite euhedra, together with rare, interstitial titanite.

Biotite hornblende micromonzodiorite (H2)
This magnetite-rich porphyritic rock contains phenocrysts of plagioclase set in a groundmass of stubby plagioclase prisms, anhedral K-feldspar, rare granular and interstitial quartz, a few scattered shreds of biotite, magnetite, accessory apatite prisms and abundant anhedra of green to yellow–green hornblende. This enclave is hosted by horn-blende–clinopyroxene quartz micromonzonite sample H7.

Dykes intruding the main pluton
Quartz latite (H22)
This hypabyssal rock is chemically a quartz syenite and appears to be a very felsic, probably highly fractionated member of the monzonitic magmas. It is rich in sodic plagioclase laths that are flow-aligned in a trachytoid fabric. The other main minerals are late, interstitial K-feldspar and very scarce quartz. Accessory phases are not evident in the thin section.

Major‐ and trace‐ element chemistry
Most of the Yzerfontein rocks (the main series) plot in the shoshonitic field in the K_2O Harker diagram (Fig. 4a), have high Ba (662–2152 ppm), high Sr (460–1951 ppm) and moderately high Zr contents (up to 406 ppm) (Electronic Appendix EA3), all characteristics typical of shoshonitic rocks. Thus, the main series is shoshonitic rather than calcalkaline. Several rocks with the highest MgO (and lowest SiO_2) contents (two olivine-bearing gabbros, J4 and M1 and a quartz diorite, H13) have low TiO_2 and CaO contents, and high MgO, Al_2O_3 and Mg#. The cumulate hornblendite (822B) is similar but, due to its cumulate character, it has low Al_2O_3 and high CaO. All these rocks plot away from the trends defined by the shoshonitic series (Fig. 4). However, with the exception of the hornblendite layer 822B, they do not appear to be strongly cumulate in character, and we interpret them as belonging to a separate high-Mg series. The fine-grained magmatic enclaves in the monzonitic rocks (plotted as blue triangles) have compositions that mirror those of their monzonitic hosts. This confirms our inference that they are autoliths—probably fragments of early chilled margins on their host magmas. The syenitic dyke rocks (plotted as green squares) essentially extend the variation trends of the monzonitic rocks toward higher SiO_2 and lower MgO contents, and the syenogranitic dykes (plotted as yellow squares) further extend this trend, though there is considerable scatter among all analysed felsic rocks (e.g., for Na_2O in Fig. 4f). The tracer isotope data (see below) suggest that the monzogranitic dykes do form part of the main shoshonitic series, and so are likely to be products of fractionation in the pluton, rather than injection of granitic magmas from external sources. Indeed, there are no exposed felsic plutons nearby (Fig. 1).

The chondrite-normalised REE patterns for most of the analysed Yzerfontein rocks (Fig. 5a, b) are similar, with ΣREE between 273 and 506 ppm, La_N/Yb_N of 10–22 and Eu/Eu* values of 0.61–0.86. One exception is the quartz microsyenite dyke (H22), which has a steeper pattern with La_N/Yb_N of 30, and a particularly steep LREE pattern, with La_N/Sm_N of 7.2; the other rocks have La_N/Sm_N in the range of 2.2–4.3.
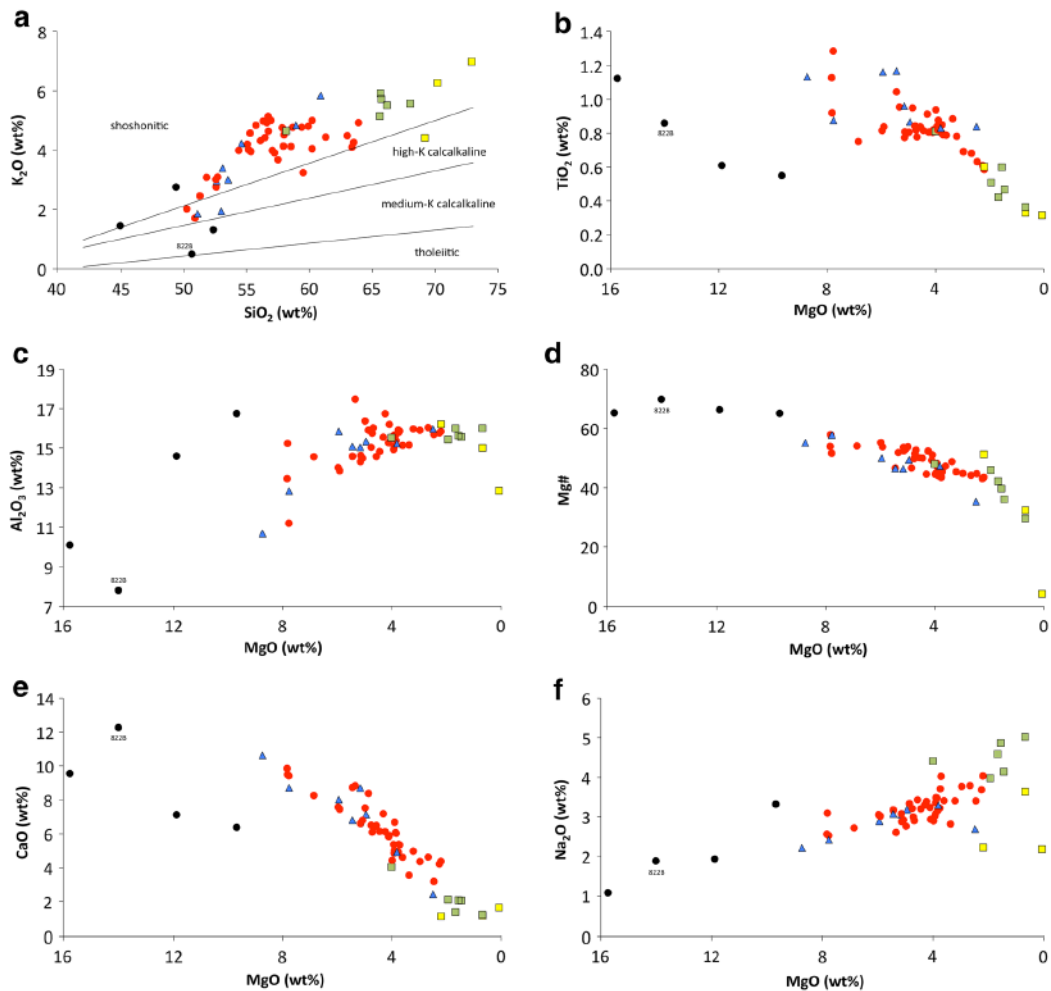
11

Fig. 4 Whole-rock, major-oxide concentrations, and Mg# [100 Mg/(Mg + Fe)] plotted against wt% MgO or SiO2 for the rocks of the Yzerfontein pluton. **a** K2O, **b** TiO2, **c** Al2O3, **d** Mg#, **e** CaO and **f** Na2O v. SiO2. Rocks of the main series are plotted as *red dots* (main pluton), *green squares* (syenitic dyke rocks) and *yellow squares* (granitic dyke rocks). The high-Mg series are plotted as *black dots* (with cumulate hornblendite 822B labelled). *Enclaves* in the rocks of the main series are plotted as *blue triangles*

The microsyenogranite dyke (H12) is distinctive in also having low ΣREE (250 ppm) and a relatively steep LREE pattern ($La_N/Sm_N = 5.0$). A further exception is the quartz diorite enclave H14, which has elevated REE contents across the spectrum (ΣREE = 694 ppm) and a significantly deeper negative Eu anomaly, with Eu/Eu* of 0.43. Despite the exceptions, all the rocks mentioned above have negative Eu anomalies and flat to slightly concave-upward HREE patterns. This suggests a general magmatic kinship. Finally, the quartz diorite H13, which belongs to the high-Mg series, exhibits a very different pattern to any of the other analysed rocks, including the hornblendite cumulate (822B) from the same series. H13 has very low ΣREE (140 ppm) and the pattern is unique in having a slight positive Eu anomaly (Eu/Eu* = 1.09). Rock H13 might, therefore, also have some cumulate character, with concentration of plagioclase.

On chondrite-normalised multi-element plots (Fig. 5b, c), all the rocks have strong, enrichments in the most mantle-incompatible elements such as Ba, Th, U and LREE, but have pronounced negative anomalies for Ta, K, Pb, P and Ti. Together with the overall shoshonitic character, this suggests a strong crustal influence on the magmas, even though

12

most were mafic to intermediate in composition and therefore must have had mantle-derived parent magmas.
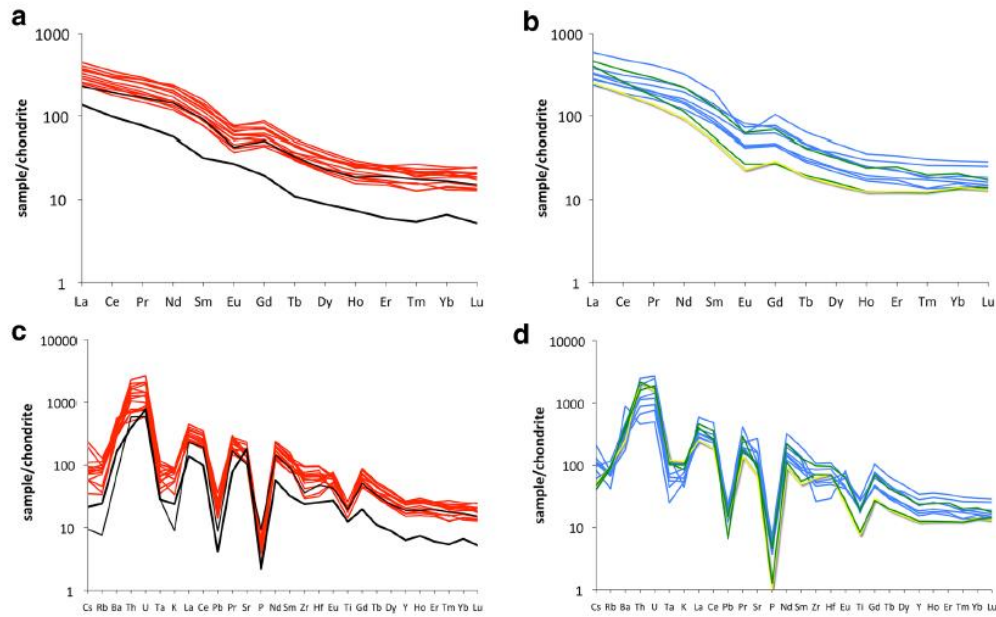

Fig. 5 a, **b** Chondrite-normalised rare-earth-element plots, and **c**, **d** chondrite-normalised multi-element spectra for the rocks of the Yzerfontein pluton. The colour coding is as given in the legend of Fig. 4, except that the *yellow line* (granitic dyke rock) has a shadow, for visibility and the lines for the syenitic dyke rocks are *dark green* here, again for visibility. The quartz diorite (sample H13) is marked with a *heavier black line*. The *normal-thickness black line* is the cumulate hornblendite (882B)

Whole‑ rock Sr and Nd isotopes

Jordaan et al. (1995) published initial $^{87}Sr/^{86}Sr$ ratios for five monzonitic to monzodioritic samples (J1, J6, J15, J16 and J27), which we have recalculated using the updated decay constant (Rotenberg et al. 2012) and our new age. To complement these, we provide new analyses for initial $^{87}Sr/^{86}Sr$ and εNd_t in two monzodiorites (H25 and H26), a monzonite (H10), a quartz monzonite (H11) and a monzonitic enclave (H24) of the main series, and a quartz diorite (H13) and a hornblendite cumulate (822B) of the high-Mg series. We also include a syenogranitic dyke that intrudes rocks of the main series (H12). Note that the rock names given to all these particular samples are based on their chemistry, as thin sections and therefore petrographic descriptions are available only for 822B, H24, H25 and H26. The Sr and Nd isotope data are provided in Table 1, in which all initial ratios have been calculated at a reference age of 535 Ma, consistent with the crystallisation age inferred from the U–Pb zircon data presented in the following section.

Figure 6a illustrates the data for initial $^{87}Sr/^{86}Sr$, plotted against MgO. The quartz diorite (H13) and the hornblendite cumulate (822B) are distinctive in having considerably lower initial $^{87}Sr/^{86}Sr$ ratios (0.70437 and 0.70430, respectively) than any of the other analysed rocks (0.70513–0.70577), confirming their separate magmatic kinships, as inferred from the elemental chemistry. Most of the rest of the monzonitic to monzodioritic rocks have initial $^{87}Sr/^{86}Sr$ ratios that cluster around 0.7056–0.7057,

13

suggesting that these are all magmatically interrelated. Monzonite J27 [analysed by Jordaan et al. (1995)] and monzodiorite H26, have lower values of 0.70532 and 0.70521, respectively. These could potentially be interpreted to represent magmas that formed as mixtures between an end member such as H13 and the main series of monzonitic to monzodioritic magmas. However, the major-oxide plots of Fig. 4 essentially rule out such an interpretation, there being no apparent mixing trends in this direction. Thus, this difference is inferred to have originated at depths below emplacement levels, possibly reflecting original heterogeneity in the inferred enriched-mantle source. Alternatively, although an enriched-mantle source is likely, given the previous subduction history of the region, this sort of difference could also be due to differing degrees of hybridisation with crust-derived magmas, at depth. As will be shown later, the zircon Hf isotope data lend apparent support to the hybridisation model. The one analysed syenogranite dyke (H12) has an initial $^{87}Sr/^{86}Sr$ ratio (0.70526) close to those of J27 and H26. Thus, the H12 magma could be modelled as a felsic differentiate of a member of the monzonitic magma suite that had undergone a little more crustal hybridisation than most.

Table 1 Whole-rock Rb–Sr and Sm–Nd isotope data for Yzerfontein samples

Sample no.	Rock-type	Rb (ppm)	$2\sigma_m$	Sr (ppm)	$2\sigma_m$	$^{87}Rb/^{86}Sr$	$^{87}Sr/^{86}Sr$	$2\sigma_m$	$^{87}Sr/^{86}Sr$ at 535 Ma	2σ
J1	Monzonite	178		777		0.663	0.71063	1	0.70566	4
J6	Monzodiorite	154		868		0.513	0.70956	2	0.70571	3
J15	Monzonite	166		810		0.593	0.71021	1	0.70576	3
J16	Monzodiorite	128		655		0.566	0.70980	2	0.70556	4
J27	Monzonite	159		891		0.516	0.70919	2	0.70532	3
H10	Monzonite	183	0.6	815	3.7	0.648	0.710567	12	0.70570	4
H11	Quartz monzonite	211	1.7	734	6.5	0.831	0.712006	10	0.70577	7
H12	Syenogranite dyke	213	0.4	441	1.1	1.397	0.715740	13	0.70526	8
H13	Quartz diorite	53	0.2	1287	1.5	0.120	0.705268	14	0.70437	1
822B	Hornblendite cumulate	16	0.3	820	19.1	0.057	0.704730	9	0.70430	1
H24	Monzonite enclave	188	1.5	948	12.6	0.575	0.709445	14	0.70513	3
H25	Monzodiorite	88	1.0	1378	30.8	0.185	0.710235	11	0.70885	2
H26	Monzodiorite	111	1.6	1458	9.1	0.219	0.706850	11	0.70521	1

Sample no.	Rock-type	Sm (ppm)	$2\sigma_m$	Nd (ppm)	$2\sigma_m$	$^{147}Sm/^{144}Nd$	$^{143}Nd/^{144}Nd$	$2\sigma_m$	εNd at 535 Ma	2σ	t_{2DM} Ga
H10	Monzonite	13.6	0.1	69.3	0.8	0.1186	0.512268	10	−1.9	0.2	1.43
H11	Quartz monzonite	12.7	0.2	66.6	0.2	0.1153	0.512268	9	−1.7	0.2	1.41
H12	Syenogranite dyke	6.73	0.10	38.8	0.4	0.1049	0.512235	11	−1.6	0.2	1.40
H13	Quartz diorite	4.40	0.08	24.2	0.2	0.1099	0.512312	13	−0.4	0.2	1.31
822B	Hornblendite cumulate	12.43	0.06	62.3	0.2	0.1206	0.512354	9	−0.3	0.2	1.30
H24	Monzonite enclave	11.24	0.09	57.1	0.8	0.1190	0.512292	15	−1.4	0.2	1.39
H25	Monzodiorite	13.78	0.14	68.3	1.5	0.1220	0.512301	12	−1.5	0.2	1.39
H26	Monzodiorite	12.54	0.28	61.4	0.1	0.1235	0.512320	13	−1.2	0.2	1.37

Samples J1, J6, J15, J16 and J27 from Jordaan et al. (1995), with $2\sigma_m$ errors of 0.2 ppm assumed for Rb and Sr concentrations
Samples H10, H11, H12, H13 822B, H24, H25 and H26 from present work

The major-oxide plots in Fig. 4 are compatible with this, as are the REE plots of Fig. 5, in which H12 has the lowest REE content of any of the analysed rocks (apart from the unrelated quartz diorite H13 and the hornblendite cumulate 822B). The one analysed enclave (micromonzonite H24) plots with the two more crustally evolved monzonitic to monzodioritic rocks, compatible with our inference that these enclaves are autoliths in the main monzonitic series. The initial Sr isotope composition of monzodiorite H25 is radically different to any of the others analysed, with an initial $^{87}Sr/^{86}Sr$ ratio of

14

0.70885. This could be interpreted as a much greater degree of interaction with radiogenic crustal materials. However, H25 is a mafic rock with SiO_2 and MgO contents (52.62 and 5.16 wt%, respectively), very similar to the other analysed monzonitic rocks (Fig. 4a and Electronic Appendix EA3). Thus, it seems more likely that the hybridising material was somewhat more radiogenic rather than the degree of hybridisation having been greater.

The Nd isotope data are illustrated in the isotope correlation plot of Fig. 6b. The monzonitic rocks, the enclave and the syenogranitic dyke all plot between −1.2 and −1.9 $\varepsilon Nd_{535\ Ma}$, which is again compatible with the suggestion that the syenogranitic magma is a differentiate from a mon-zonitic parent and that the enclaves are autoliths. Unlike its Sr isotopic composition, the $\varepsilon Nd_{535\ Ma}$ value for mon-zodiorite H25 (−1.5) is essentially the same as the other rocks of the monzonitic series. This suggests that whatever crustal interaction resulted in the elevated initial $^{87}Sr/^{86}Sr$ ratio, it affected the Nd isotope system very little. This decoupling of the isotope systems suggests that the process of hybridisation did not involve bulk assimilation of crust but perhaps rather interaction with a melt derived from a crustal rock. As for the Sr isotope ratio, the $\varepsilon Nd_{535\ Ma}$ values (−0.4 to −0.3) of the quartz diorite (H13) and the hornblendite cumulate (822B) are quite distinct, suggesting a less radiogenic mantle source, and/or far less interaction between these magmas and crustal rocks or magmas. The depleted-mantle Nd model ages of all the Yzerfontein rocks lie between 1.30 and 1.43 Ga (Table 1). In view of the likelihood of mantle enrichment and the contribution from detrital zircon crystals derived from Malmesbury Group and Swartland complex, we consider it likely that these ages reflect a rather uniform degree of mixing between mantle and crustal sources during the formation of the Yzerfontein magmas. Since the less radiogenic rocks of the high-Mg series have essentially the same Nd model ages as the more evolved shoshonitic series, this suggests that partial melting of enriched mantle probably dominated over later crustal assimilation.
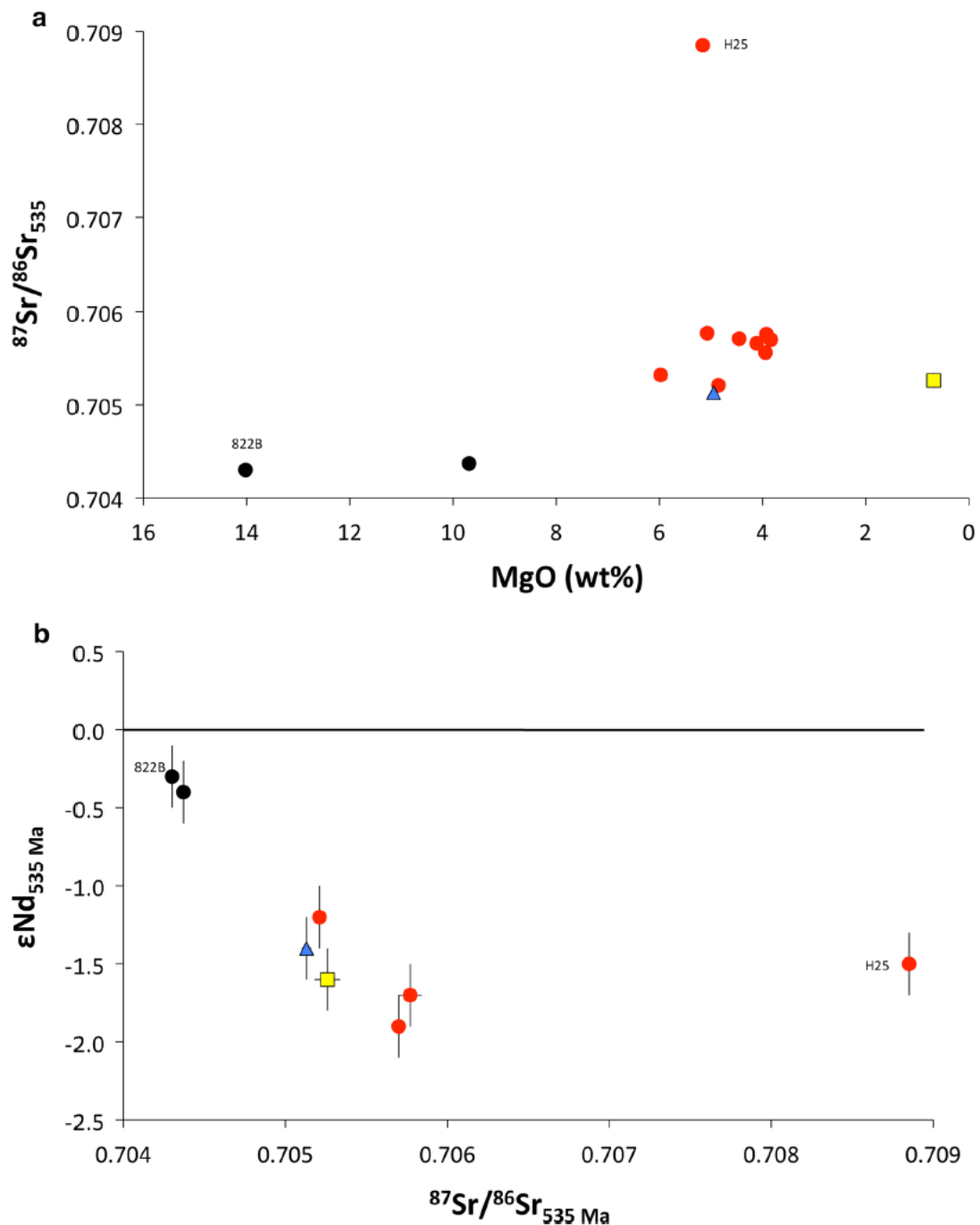
Fig. 6 Diagrams illustrating the Sr and Nd isotope variations in the rocks of the Yzerfontein pluton, **a** initial $^{87}Sr/^{86}Sr$ plotted against MgO (wt%), **b** εNd_t plotted against initial $^{87}Sr/^{86}Sr$. The colour coding is as given in Fig. 4, with the hornblendite cumulate rock (822b) and monzodiorite H25 labelled. In **a**, the 2σ *error bars* for initial $^{87}Sr/^{86}Sr$ are plotted but are all smaller than the plot symbols. The same is true in **b**, except for quartz monzonite (H11) and micromon-zogranite H12 (*yellow square*)

Zircon U–Pb data

LA-SF-ICP-MS U/Pb zircon geochronology was undertaken on four samples: H10 (monzonite), H11 (quartz monzonite), H12 (syenogranite dyke) and H13 (quartz diorite from the high-Mg series). Figure 7 illustrates the morphologies and internal zoning patterns of the analysed zircon crystals. Zircon grains in the four samples are subhedral to euhedral and prismatic, typically 75–200 μm long, with aspect ratios of 2–4. Statistically, the most elongate zircon crystals occur in H13 (quartz diorite) and the most equant in H12 (syenogranite dyke). In cathodoluminescence images, the zircons

16

from H10, H11 and H12 commonly show broadly zoned, CL-dark to -intermediate euhedral centres and concordant fine, and euhedral oscillatory-zoned mantles (H10, H11 and H12). Zircons from H13 show broad, planar banding that is typically dark to intermediate in CL. The zoning patterns and grain shapes suggest that all these represent magmatic zircons. Zircon grains from samples H10, H12 and H13 additionally contain anhedral xenocrystic cores of variable but generally bright CL response, commonly rimmed by CL-dark mantles. Xenocrystic zircon was not observed in H11.

U–Pb isotope data from the magmatic oscillatory-zoned mantles, euhedral centres and broadly banded zones are interpreted to date the emplacement of the magmas. The magmatic zircon domains from H10 to H13 yield Concordia ages of 535 ± 3 Ma [2σ, MSWD of concordance and equivalence (C + E) = 0.55], 537 ± 3 Ma [2σ, MSWD (C + E) = 1.8], 535 ± 3 Ma [2σ, MSWD (C + E) = 1.13] and 533 ± 3 Ma [2σ, MSWD (C + E) = 0.80], respectively. These are all identical, within error (Figs. 8, 9; Electronic Appendix EA4). Magmatic growth zones that yield these ages have a wide variation in U contents (145–3293 ppm) and Th/U (H10 = 0.53–1.18, H11 = 0.15–0.65, H12 = 0.46–0.86 and H13 = 0.02–0.48; Electronic Appendix EA4). Uncertainties on the concordia ages are <1% relative for all samples, probably due to the relatively large number of analyses carried out. Given that high-spatial-resolution techniques such as LA-ICP-MS or SIMS are typically thought to yield ages with a precision of ~1% relative, the quoted uncertainties are likely to some- what under-estimate the true uncertainty (e.g. Rosenbaum et al. 2012). Taken together, the U–Pb zircon chronology suggests that the crystallisation age of the Yzerfontein magmas was synchronous at c. 535 Ma. This age has been used as the reference age for radiogenic tracing datasets (see above). Note that our new crystallisation age for Yzerfontein is significantly older than the c. 519 Ma age previously determined by Jordaan et al. (1995); see below.
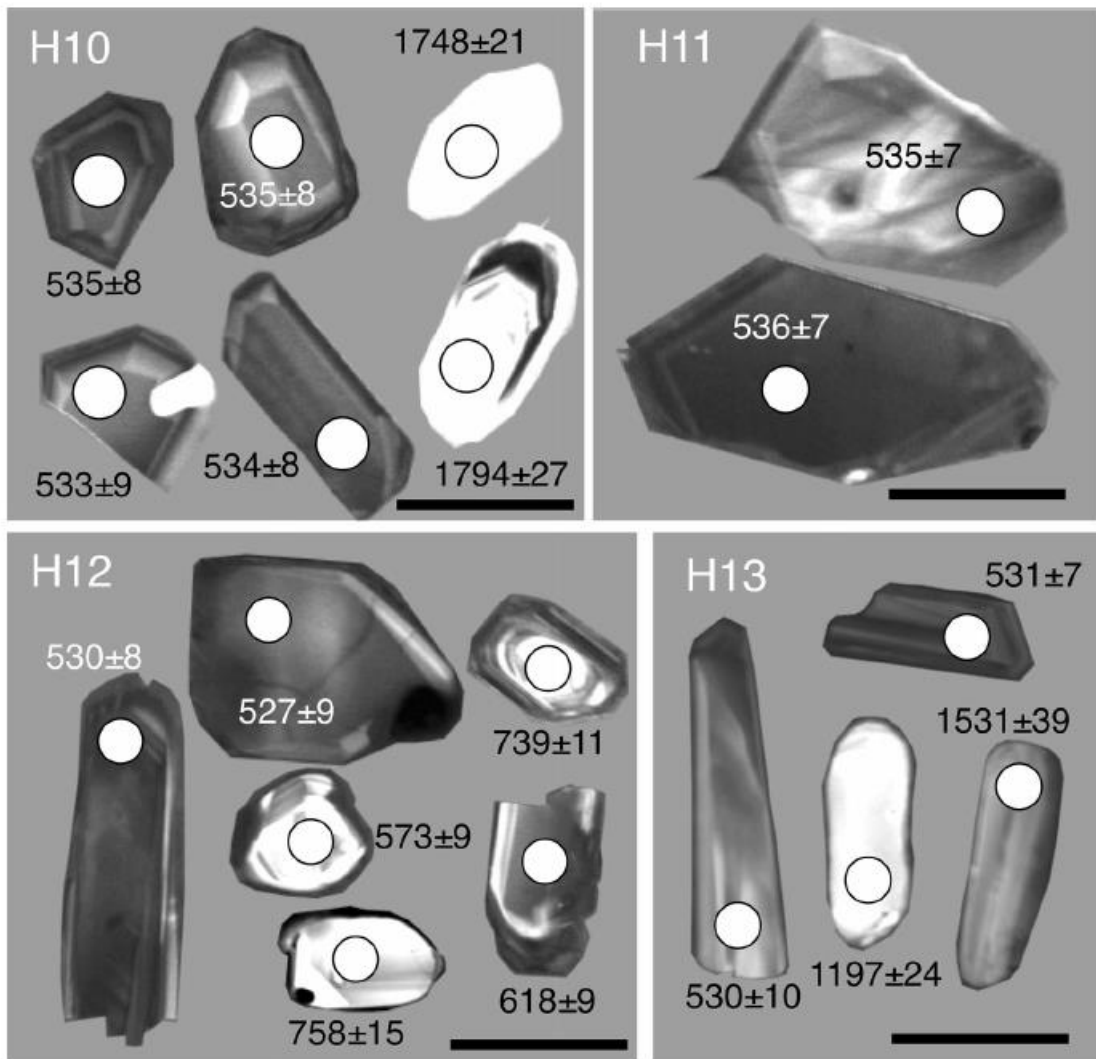
Fig. 7 Cathodoluminescence images of representative zircon grains from the Yzerfontein pluton, sample H10 (monzonite of the main series), sample H11 (quartz monzonite of the main series), sample H12 (a syenogranite dyke intruding rocks of the main series) and sample H13 (quartz diorite of the high-Mg series).

U–Pb Analytical spots are shown, together with the apparent ^{207}Pb-^{206}Pb (>1200 Ma) or ^{206}Pb-^{238}U (<1200 Ma) spot ages) in Ma, with 2σ uncertainties. In each figure the *scale bar* is 100 μm. Wetherill concordia diagrams are given in Figs. 8 and 9. See text for further details and description
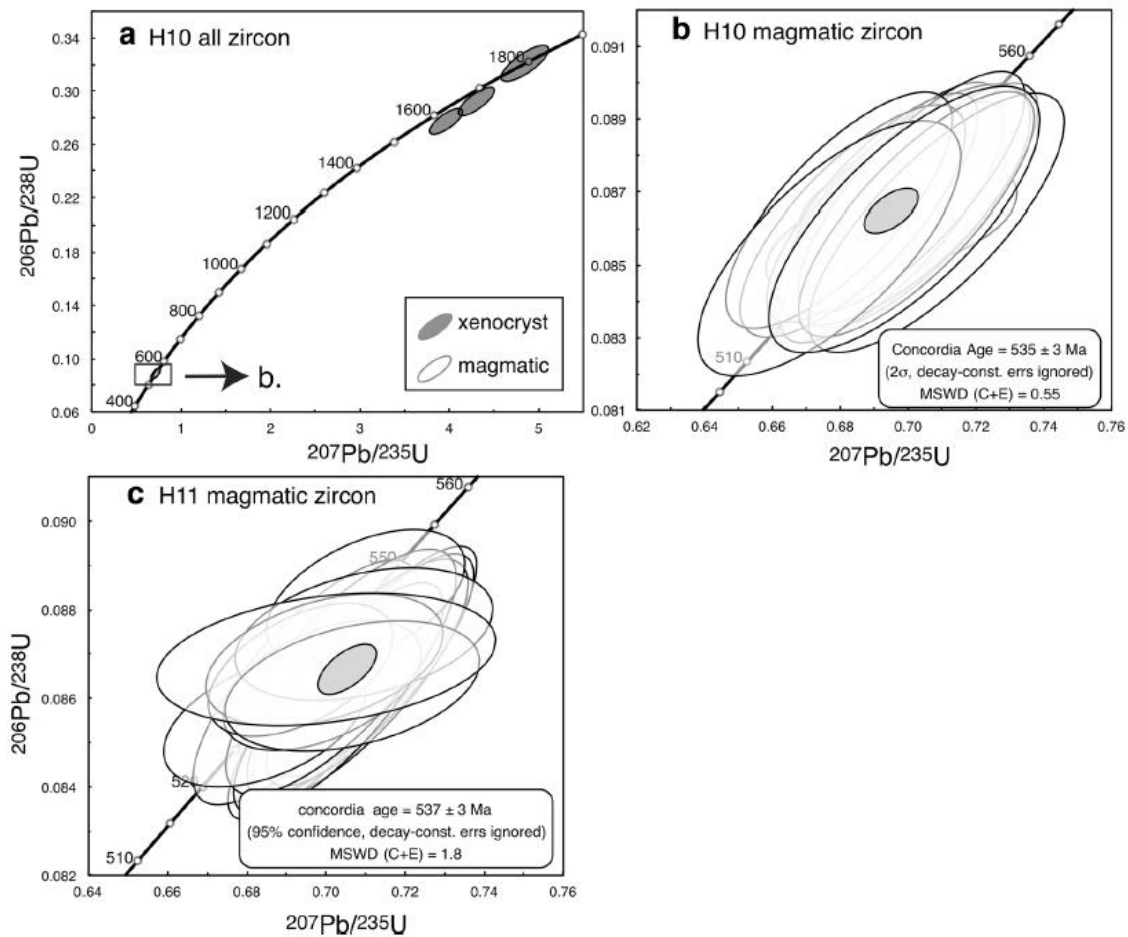
Fig. 8 Wetherill concordia diagrams for Yzerfontein samples H10 (**a**, **b**) and H11 (**c**). Data-point error ellipses are 2σ

Xenocrystal zircon cores commonly show bright CL responses. The three analyses from H10 (monzonite) are concordant to slightly discordant (100 to 93%, based on agreement between $^{206}Pb/^{238}U$ and $^{207}Pb/^{206}Pb$ ages) and have apparent spot $^{207}Pb/^{206}Pb$ ages in the range 1694 ± 24 Ma (2σ) to 1794 ± 26 Ma (2σ; Fig. 8). In H12 (syenogranite dyke) most analyses (25 of 28) of xenocrystal zircon are >90% concordant, and spread out along the concordia, with apparent spot ages that range from 1863 ± 34 Ma (2σ) to 557 ± 16 Ma (2σ; Fig. 9). Most of the concordant ages are <900 Ma, with clusters of ages, as determined by mixture modelling (Sambridge and Compston 1994), at c 0.58, 0.63, 0.72 and 0.83 Ga. From Sample H13 (high-Mg series quartz diorite) 14 of 21 analyses of xenocrystal zircon were >90% concordant, with apparent spot ages between 1555 ± 58 Ma (2σ) and 609 ± 18 Ma (2σ; Fig. 8, Electronic Appendix EA4). The concordant analyses show some clustering of ages at c. 0.65, 1.1, 1.2 and 1.5 Ga. The remainder are discordant, the oldest having an apparent $^{207}Pb/^{206}Pb$ spot age of 1745 ± 36 Ma (2σ). Thus, three of the four analysed Yzerfontein samples contain inherited/ xenocrystal zircon crystals that have a range of ages that broadly match the inheritance in the CGS S-type granites and detrital zircon population from the Malmesbury Group metasediments (Villaros et al. 2012). This suggests that an evolved crustal component was physically incorporated into some of the Yzerfontein magmas.

19

Zircon Lu–Hf data

Seventeen Hf isotope analyses were carried out on the magmatic zircon domains in H10 (main series monzonite). They show a narrow range of $\varepsilon Hf_{535\,Ma}$ from -0.6 ± 0.8 (2σ) to $+0.8 \pm 0.6$ (2σ), consistent with a narrow range of two-stage, late Mesoproterozoic, depleted-mantle, Hf model (t_{2DM}) ages (1.22 to 1.14 Ga; Electronic Appendix EA5). In addition, three inherited cores, with $^{207}Pb/^{206}Pb$ spot ages of c. 1.79 to 1.69 Ga, yielded less radiogenic Hf isotope compositions at their time of crystallisation (εHf_t = +5.5 to +8.3) and Palaeoproterozoic t_{2DM} model ages (1.84 to 1.76 Ga; Electronic Appendix EA5). Zircon Hf isotope compositions from magmatic domains in H11 (main series quartz monzonite) overlap with those of H10 ($\varepsilon Hf_{535\,Ma}$ from -1.1 ± 0.7 (2σ) to $+1.1 \pm 0.6$ (2σ), n = 13) and yield similar, Late Mesoproterozoic depleted-mantle model ages (t_{2DM} = 1.25 to 1.13 Ga; Electronic Appendix EA5).
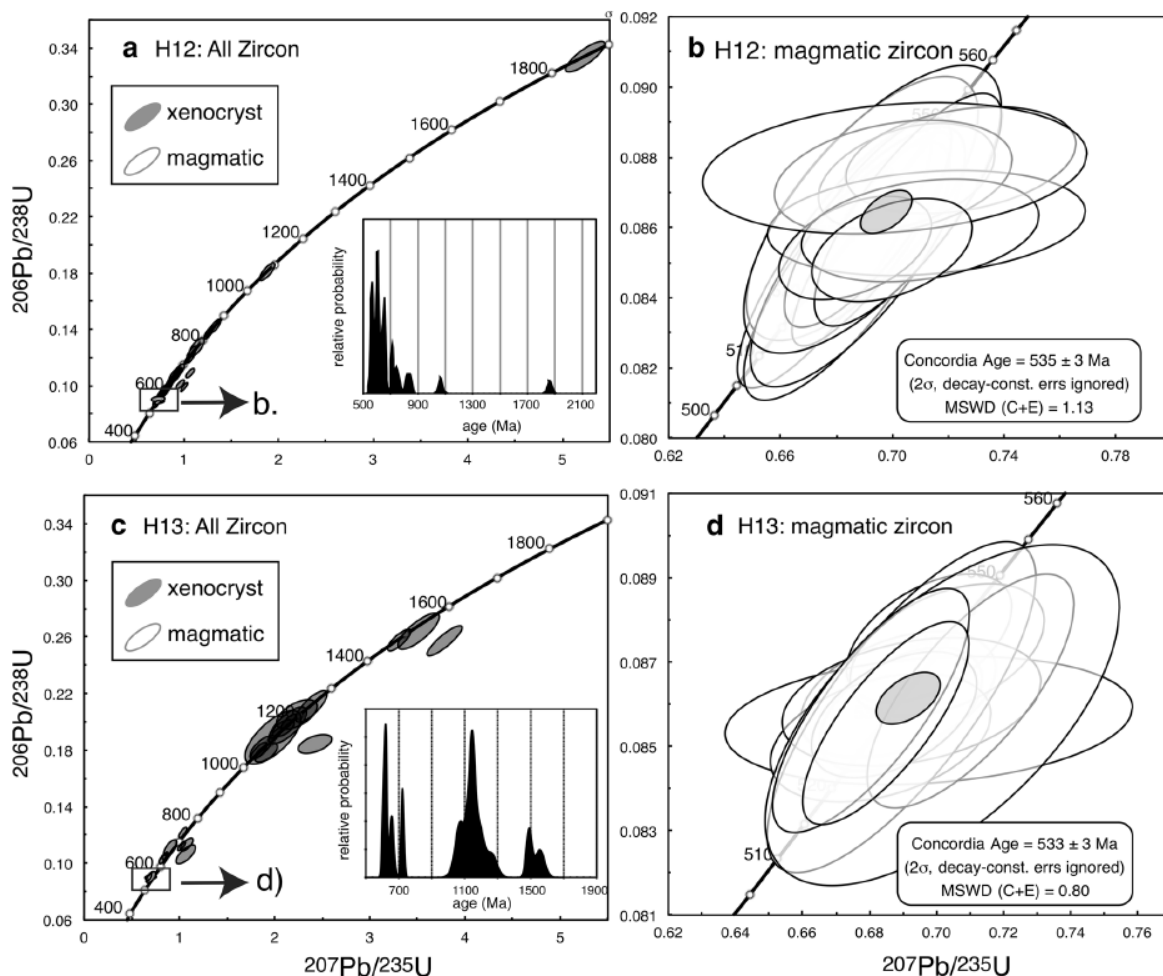
Fig. 9 Wetherill concordia diagrams for Yzerfontein samples H12 (**a, b**) and H13 (**c, d**). *Insets* in **a, c** show relative probability distributions for ≤10% discordant analyses of xenocrystic zircon. Data-point error ellipses are 2σ

Samples H12 (shoshonitic series) and H13 (high-Mg series) contain much higher proportions of xenocrystal zircon cores than H10 and H11. Magmatic zircon domains in H12 (syenogranite dyke) overlap the least radiogenic compositions of magmatic zircons in H10 and H11, but also record significantly lower (more evolved) values

20

(εHf$_{535 \text{ Ma}}$ = −3.6 ± 0.6 (2σ) to +1.1 ± 0.7 (2σ); n = 17; Electronic Appendix EA5). Depleted-mantle model ages define a narrow range (t_{2DM} = 1.38 to 1.13 Ga; Electronic Appendix EA5). Xenocrystal cores show a wide range of εHf$_t$ values at their times of crystallisation, ranging from −1.2 ± 0.6 (2σ) to +11.0 ± 0.5 (2σ). However, with one exception (t_{2DM} = 2.30 Ga), the xenocrysts show a range of depleted-mantle Hf model ages (t_{2DM} = 1.29 to 0.82 Ga) that overlaps the range obtained from the magmatic zircon (Electronic Appendix EA5).

Compared with the other rocks, magmatic zircons from H13 (high-Mg series quartz diorite) have the widest range of Hf isotope compositions (εHf$_{535 \text{ Ma}}$ = −8.0 ± 0.8 (2σ) to −0.5 ± 0.5 (2 s); n = 9; Electronic Appendix EA5) and, overall, the most radiogenic isotope compositions. They yield somewhat older Mesoproterozoic depleted-mantle Hf model ages (t_{2DM} = 1.63 to 1.21 Ga; Electronic Appendix EA5) than magmatic zircons from the other samples. Xenocrystal zircon cores also show a wide range of compositions, with some Late Mesoproterozoic domains having highly positive εHf$_t$ (Electronic Appendix EA5). Two-stage depleted-mantle Hf isotope model ages for the xenocrystal zircons range from 3.10 to 1.11 Ga.

Magmatic zircons from the Yzerfontein rocks show nearly the same range of Hf isotope compositions as magmatic zircons from coeval S-type CGS granitic rocks (Fig. 10; Villaros et al. 2012). Xenocrystal zircon cores from Yzerfontein have ranges of spot ages and Hf isotope compositions that partially overlap with those of xenocrystal zircons from the S-type granites. However, overall, they are somewhat less isotopically radiogenic at any given inferred age (Fig. 10). Similarly, Yzerfontein xenocrystal zircon cores of Neo-proterozoic to Mesoproterozoic age overlap the Hf isotope compositions of all but the most radiogenic detrital zircons of comparable age from the Malmesbury Group metasedimentary rocks (Fig. 10; Frimmel et al. 2013).

Villaros et al. (2012) interpreted the wide range in Hf isotope compositions from magmatic zircon domains in any given sample of CGS S-type granite to reflect inefficient homogenisation of Hf that had been derived from the dissolution of isotopically heterogeneous populations of xenocrystal zircon. The four Yzerfontein samples show a positive correlation between the abundance of xenocrystal zircons and the range of magmatic Hf isotope compositions. This suggests that a similar mechanism to that proposed by Villaros et al. may control Hf isotope heterogeneity in magmatic zircon from Yzerfontein. Xenocrystal zircon cores in the Yzerfontein magmas appear to have a similar origin to the cores from the inherited zircon crystals in the CGS S-type granites. Therefore, it is reasonable to suggest that they are derived from the same source, i.e., metasedimentary rocks of the Malmesbury Group and Swartland complex.

Discussion
Age and tectonic context
The U–Pb age data indicate that there are no significant differences in the magmatic crystallisation ages for different magmatic phases of the Yzerfontein pluton. Our new crystallisation age is around 10 to 15 Myr older than a previous TIMS age determination that used multiple grains obtained from five samples ranging in composition from

monzonite to monzogabbro. Those isotopic data for the different zircon fractions dated by TIMS were either weakly normally or reversely discordant and yielded an upper intercept age of 519 ± 7 Ma [MSWD = 0.705; Jordaan et al. (1995)].
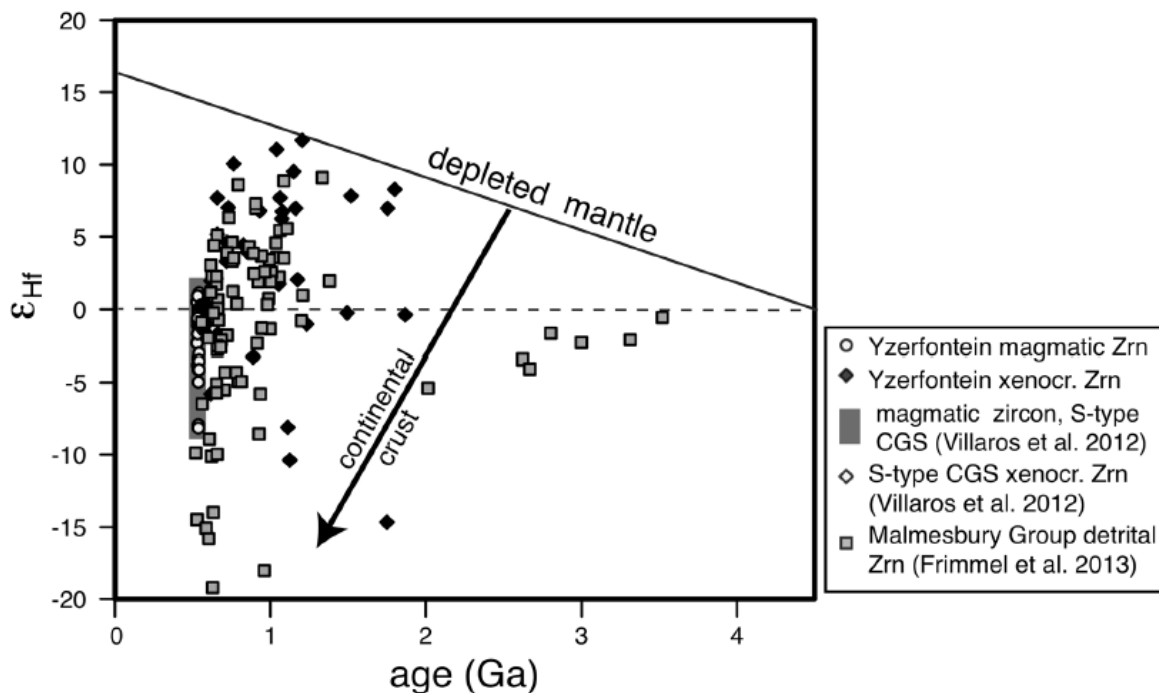

Fig. 10 Zircon hafnium isotope compositions (expressed as εHf$_t$) v. age for magmatic mantles and xenocrystal cores from the Yzerfontein rocks. For comparison, data are shown for detrital zircons from the Malmesbury Group (Frimmel et al. 2013) and xenocrystal zircon cores in CGS S-types granites (Villaros et al. 2012). The range of εHf$_t$ values of magmatic zircon mantles from the S-type CGS granites (Villaros et al. 2012) is shown as a *dark grey shaded box*. The continental crustal evolution vector assumes that $^{176}Lu/^{177}Hf$ = 0.0113 (Wedepohl 1995). The isotopic evolution of the depleted mantle is assumed to be linear with time, from εHf = 0 at 4.58 Ga to εHf = +16.4 at the present day. It was calculated assuming that the present-day depleted mantle has the following isotope ratios: $^{176}Lu/^{177}Hf$ = 0.0384 and $^{176}Hf/^{177}Hf$ = 0.28325 (Griffin et al. 2002)

Our new U–Pb age determinations firmly link the emplacement age of the Yzerfontein mafic to intermediate monzonitic magmas with the emplacement of the c. 550–520 Ma, late syntectonic, high-K, I- and S-type granitic rocks of the CGS (Da Silva et al. 2000; Armstrong et al. 1998; Villaros et al. 2012), rather than to the 525–510 Ma A-type plutonism (Scheepers and Poujol 2002; Chemale et al. 2011).

Although the collective number of U–Pb isotope analyses of xenocrystal zircon from the four samples is relatively small, concordant ages cluster at c. 0.6–0.8 Ga and c. 1.2–1.0 Ga, with a few Mesoproterozoic or Palaeoproterozoic cores. This age distribution is broadly similar to that obtained for xenocrystal zircon from S-type CGS granites (Villaros et al. 2012), and for detrital zircons from silici- clastic sediments in the Malmesbury Group and Swartland complex (Frimmel et al. 2013).

Kisters et al. (2015) used inferences based on the structure of the Saldania Belt to infer that the latest Proterozoic to early Cambrian crustal magmatism here was triggered by either subduction of a mid-oceanic ridge or the opening of a slab window, allowing

upwelling of the deep hot mantle. In either case, our new 535 Ma date for the Yzerfontein mafic to intermediate magmatism is in accord with this sort of event having provided the heat source for high-grade metamorphism of the deep crust and partial melting of both the enriched-mantle wedge and the overlying crust, to produce the late syntectonic magmatism of the CGS. In the sections below, we address a number of issues relating to the genesis of the Yzerfontein pluton.

Magmatic kinships tectonic settings and petrogenetic relationships

Jordaan et al. (1995) used a Ti–Zr–Y plot (Pearce and Cann 1973) of the more mafic rocks that they analysed, to infer that the magmas were not within-plate-related but plot in the fields of ocean-floor and calc-alkaline basalts. As concluded by Dudás (2012, p. 13261) "If geochemical processes unrelated to subduction are involved, trace-element discrimination diagrams are misleading and are inadequate criteria for interpreting the tectonic environment." Given that the magmatism concerned was late- to post-collisional in character, we should probably not attach great significance to the indications from such discrimination plots.

Jordaan et al. (1995, p. 68) write that "The age, as well as the major- and trace-element geochemistry of the mafic and intermediate rocks are, therefore, compatible with the interpretation that the Yzerfontein and Mud River plutons are the mafic and intermediate counterparts of a potassic trans-alkaline (high-K calcalkaline) series with the younger I-type Cape granites (Scheepers 1995) within the Swartland terrane perhaps being the felsic end-members". As we will see below, this cannot be the case. However, even on geographical grounds, this idea seems unlikely, since the I-type granites of the CGS occur only on the northeastern (opposite) side of the Colenso Fault (Fig. 1). A primary interpretation of these geographical relations would be that suitable protoliths for I-type granitic magmas are absent in the crustal segment where the Yzerfontein pluton is located, on the southwestern side of the Colenso Fault.

What is certain is that the rocks of the Yzerfontein pluton belong mainly to the shoshonitic series, being highly enriched in LILE (Cs, Ba, Rb, Th, K, U), LREE and MREE. The shoshonitic character should not be interpreted as indicating a particular tectonic environment either, but rather as a product of the chemical and mineralogical characteristics of the enriched-mantle source rocks for the magmas, combined with possible direct hybridisation with crustal materials. The 535 Ma age is similar to those of the CGS S- and I-type felsic magmatism; so it is certainly relevant to the question of whether the Yzerfontein magmas are related to those of the I-type granitic rocks of the CGS. Figure 11 shows that there are clear differences between Yzerfontein and CGS I-type rocks. Yzerfontein rocks are very much more potassic (Fig. 11a, shoshonitic as against high-K calc- alkaline for the I-type granitic rocks), and there are also clear contrasts in the variations in CaO and Na_2O (Fig. 11 b, c). Figure 12 illustrates the ranges of $\varepsilon Nd_{535\ Ma}$ for the I-type granitic rocks of the CGS (Chemale et al. 2011) and the Yzerfontein pluton (present work). Note that there is little overlap between the two datasets, with the CGS I-types having significantly more radiogenic Nd isotope signatures (lower $\varepsilon Nd_{535\ Ma}$).

The data cited above show that the shoshonitic magmas of the Yzerfontein pluton have no magmatic relationship with the coeval granitic magmas. Partial melting of mafic, intermediate or silicic crustal rocks, at temperatures up to 1000 °C, will result in formation of a variety of highly felsic melts [e.g., Clemens (2006)], and essentially granitic magmas. We also have no evidence for the presence of pre-existing crust here with the required Sr and Nd isotopic characteristics. Thus, any model that sought to derive the monzonitic magmas of the Yzerfontein pluton through direct crustal melting would not be credible.

Due to the potassic character of the Yzerfontein rocks, it could be hypothesised that the Yzerfontein magmas represent assimilation of Malmesbury Group or Swartland complex metasediments by a mantle-derived magma or that there may have been some kind of mixing between a mantle-derived parent magma and partial melts derived from these crustal materials. The CGS S-type magmas are inferred to represent partial melts of deep Malmesbury Group or Swartland complex metasediments, with some entrainment of peritectic minerals (e.g. Stevens et al. 2007; Villaros et al. 2009; 2012). Figure 13 shows isotope plots that illustrate the possible and impossible genetic relationships between the Yzerfontein pluton, the CGS S- and I-type granitic rocks, and the rocks of the Malmesbury Group. Figure 13b shows that there is no overlap in Nd and scant overlap in Sr isotopic composition between the analysed Yzerfontein materials and any other group of rocks. Reinforcing our observations, based on elemental concentrations (e.g. Figure 11), Fig. 13a also shows that there are no Sr isotope mixing lines between the cluster of Yzerfontein points and either the Malmesbury Group rocks or the CGS granites. Thus, we conclude that there are no direct magmatic links between the Yzerfontein rocks and the granitic rocks of the CGS, nor is there any Nd or Sr isotope evidence that the Yzerfontein magmas derived their main crustal components through assimilation of Malmesbury Group rocks.
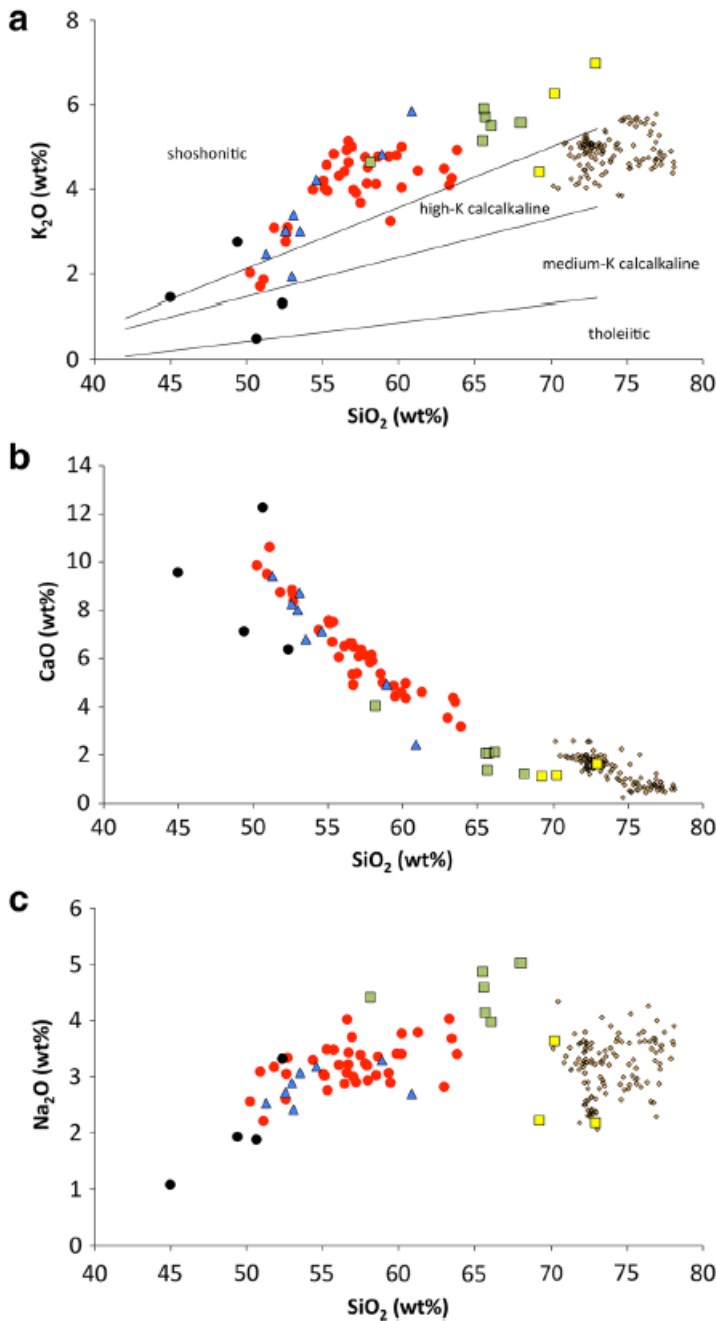
Fig. 11 Harker diagrams illustrating the chemical contrasts between the rocks of the Yzerfontein pluton (symbols as in Fig. 4) and the I-type granitic rocks of the Cape Granite Suite (CGS, small diamonds), **a** K2O, **b** CaO and **c** Na2O. Data for the CGS taken from a compilation in Villaros (2010)

Nevertheless, our U–Pb and Hf isotope data show that the Yzerfontein rocks contain an inherited zircon population that is plausibly derived from a source that contains detrital zircons whose age distribution is broadly similar to that of the Malmesbury Group and the Swartland complex. This relationship suggests that there must have been some physical and/or chemical assimilation of such metasedimentary materials, in addition to magma derivation from an enriched-mantle source. As shown earlier, bulk assimilation is unlikely, so one suggestion would be partial melts of rocks similar to the Swartland complex, and carrying some entrained restitic zircons, mixed with the mantle-derived magmas to produce or modify the shoshonitic magmas. As shown above, sample H13, a member of the high-Mg series also contains numerous inherited cores in its

25

zircon population. This suggests that interaction with crust-derived materials must have occurred in all the magmas of the Yzerfontein pluton, even in the most Mg-rich and Si-poor types. The amounts of assimilation that might be required are modelled later, in the section on crustal assimilation.

Evidently, the pluton was emplaced broadly synchronously with some of the early S-type CGS magmas; so it is possible (even probable) that the Yzerfontein magmas represent a low-volume, high-level expression of the mantle magmatism that is inferred to have caused partial melting of the crust and production of the CGS granites. As is clear from various chemical and isotope plots (Figs. 11, 12, 13), the Yzerfontein and CGS I-type granitic magmas do not share close magmatic kinships, and do not form parts of any single mixing or fractionation lineage.

A further question is whether the parent magmas for the Yzerfontein pluton were akin to alkali basalts derived from enriched subcontinental mantle, but this seems unlikely. Figure 14 shows a plot of TiO_2 against FM (FeO^T + MnO + MgO), in which it is clear that the TiO_2 contents of the Yzerfontein rocks are too low for them to have had normal alkali basaltic parent magmas.

The evidence presented here strongly suggests that some differentiation occurred within the various batches of Yzerfontein magmas. The numerous fine-grained autolithic enclaves, many of them more mafic than the enclosing rocks, and the cross-cutting dykes of related granitic to syenitic rocks all suggest that crystal fractionation operated, at least locally. However, at the present level of exposure, there are no overt signs of such a fractionation process. Thus, we suggest that, like the possible hybridisation, fractionation events probably occurred at deeper levels.
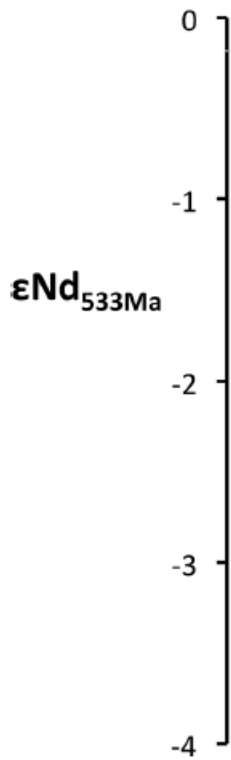
Fig. 12 Plot showing the ranges of εNdt for the I-type granitic rocks of the Cape Granite Suite (CGS, *blue diamonds*) and the rocks of the Yzerfontein pluton (*red squares*), calculated at a reference age of 535 Ma. The CGS points were recalculated from data presented in Chemale et al. (2011). The 2σ *error bars* represent assumed values of ±0.2 epsilon units. This plot illustrates the generally higher εNdt values for the Yzerfontein rocks and the limited degree of overlap in the two data sets

Mantle protolith

Although the parental magmas for the Yzerfontein pluton were not common basaltic types (e.g., Figure 14), the mafic to intermediate chemistry of the majority of the rocks, and the fine-grained texture (quenched liquid character) of some, strongly suggests a mantle source. The initial $^{87}Sr/^{86}Sr$ of the majority of the mafic to intermediate Yzerfontein rocks lies close to values for highly enriched mantle, similar to the postulated EM2 reservoir (around 0.706). Given the likely fore-arc setting of the Malmesbury Group rocks that were deposited just prior to the CGS magmatism, this suggests a mantle wedge source that had been enriched (metasomatised) by slab-derived fluids, probably to such an extent that it was no longer peridotitic but dominated by rock types such as phlogopite clinopyroxenite (e.g., Wyllie and Sekine 1982; Enggist and Luth 2016). Nevertheless, the mantle here must have been variably enriched because quartz diorite sample H13 is more magnesian, has the lowest degree of inferred enrichment of any of the analysed mafic rocks (except the cumulate hornblendite 822B, Fig. 4) and, together with 822B, has a far more primitive initial $^{87}Sr/^{86}Sr$ (near 0.704, Fig. 6). As inferred earlier, H13 appears to belong to a separate group of magmas characterised by high MgO and Mg#, Al_2O_3, Na_2O, and low TiO_2 and CaO, suggesting that, as might be expected, the mantle here contained some domains that escaped extensive metasomatic enrichment.

Crustal assimilation

Despite the relationships shown in Fig. 13, and the discussion above, it might be hypothesised that intermediate members of a putative mixing series between partial melts of metasediments and tholeiitic to alkaline basaltic magmas might simply be missing from the exposed geology but exist at depth. As explained earlier, the known basement rocks in the in this part of the Saldania Belt are mainly metasediments belonging to the Malmesbury Group and the Swartland complex (Fig. 1). Thus, we can test whether the crustally enriched character of the Yzerfontein magmas could have arisen through assimilation of Malmesbury Group rocks by mantle-derived mafic magmas. In doing so, we found that the Nd and Sr isotope characteristics of the Yzerfontein magmas can indeed be modelled by assimilation of about 14% of a felsic partial melt derived from Malmesbury Group metasediments by an assumed mantle-derived parent magma with SiO_2 of 50 wt%, initial $^{87}Sr/^{86}Sr$ of about 0.703 and $\varepsilon Nd_{535\ Ma}$ of about –1.0. However, given that the crustal melt would have contained about 73 wt% SiO_2 (typical for partial melts of metasedimentary protoliths of pelitic to greywacke composition; Clemens and Stevens 2012), 30% assimilation would be required to obtain a hybrid with 57 wt% SiO_2—more than twice the amount needed to balance the isotope equation. The TiO_2 balance also shows that such a model is non-viable. An alternative could be bulk assimilation of a Malmesbury metapelite. This type of model has already been discounted on the basis of the decoupling of the Sr and Nd isotope systems but can also be ruled out because the Malmesbury Group metasediments (Electronic Appendix EA3) have 68–70 wt% SiO_2, and thus over 35% assimilation would be required to arrive at a target SiO_2 content of 57 wt%. To model assimilation using the Sr isotope system, we assume that the basaltic end member has 1400 ppm Sr (similar to Yzerfontein gabbro sample J4, Electronic Appendix EA3), with $^{87}Sr/^{86}Sr_{535Ma}$ of 0.7043 (similar to cumulate rock 822B or high-Mg series quartz diorite H13, Table 1). For the Malmesbury Group or Swartland complex assimilant, we use a Sr content of 70 ppm (Electronic Appendix EA3) and $^{87}Sr/^{86}Sr_{535Ma}$ of 0.716 (Fig. 13a).
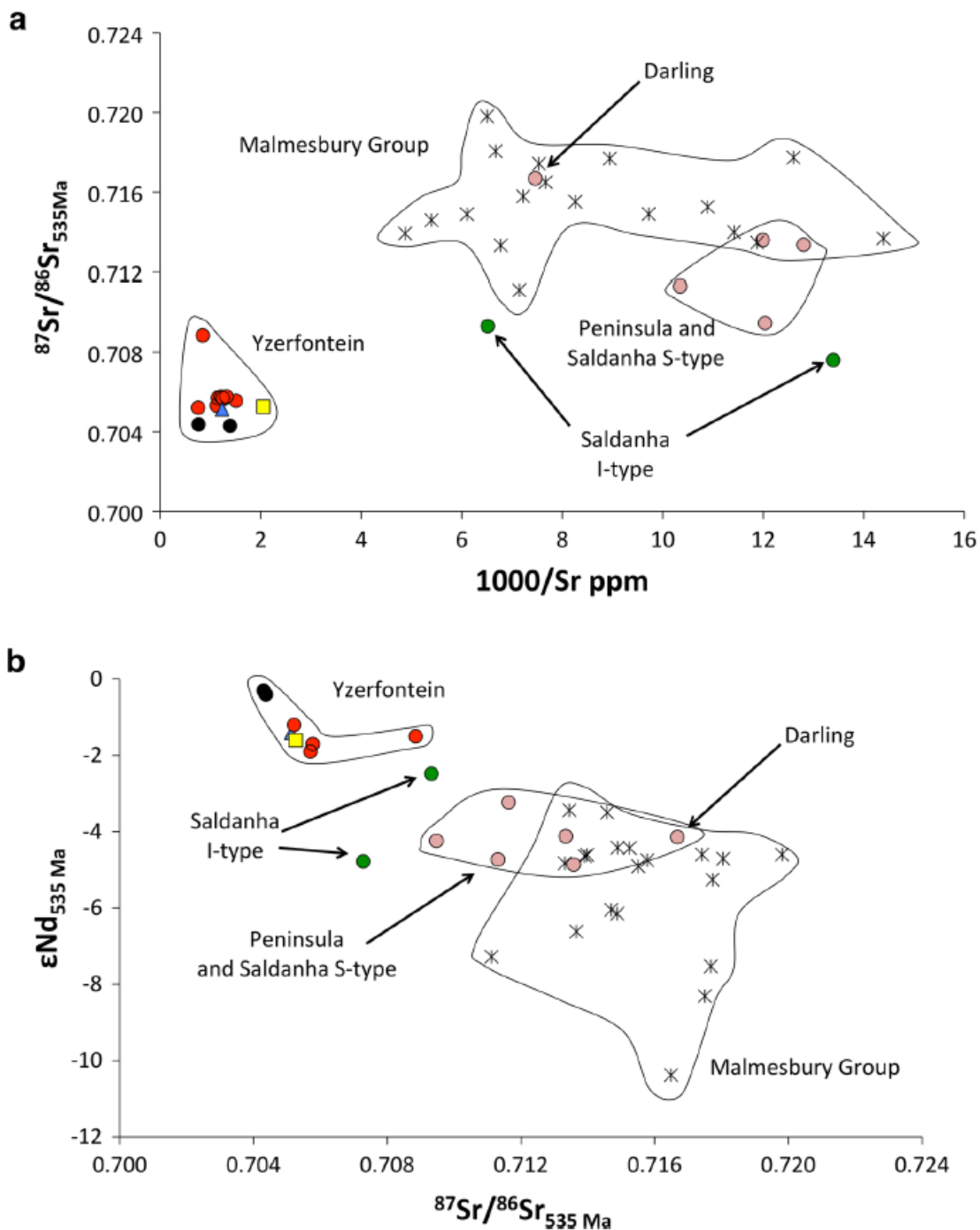
Fig. 13 Isotope plots illustrating the relationships between the rocks of the Yzerfontein pluton, the Cape Granite Suite (CGS) S-type (*pink dots*) and I-type (*dark green dots*) granitic rocks and the metasedimentary rocks of the Malmesbury Group (*stars*), with all isotope ratios normalised to the new 535 Ma age for the Yzerfontein pluton, **a** Sr isotope mixing plot, with initial $^{87}Sr/^{86}Sr$ plotted against 1000/Sr, **b** isotope correlation diagram, with εNd_t plotted against initial $^{87}Sr/^{86}Sr$. See text for data provenance and discussion

To satisfy the Sr isotope constraints and produce the monzonitic rock with 850 ppm Sr and $^{87}Sr/^{86}Sr_{535Ma}$ of 0.7057 (Electronic Appendix EA3; Table 1) would require assimilation of >70 wt% of metasediment. Quite apart from the gross mismatch between the elemental and isotopic requirements, this is clearly a preposterous degree of assimilation. The model would be even less viable if the parental basaltic end member

29

was alkaline instead of tholeiitic, the assimilant poorer in SiO_2 or with a lower initial Sr isotope ratio. Similarly, if one considers another important major oxide, TiO_2 for example, the Malmesbury Group and Swartland complex metasediments contain an average of around 0.9 wt% (Electronic Appendix EA3). A basaltic magma with about 0.6 wt% TiO_2 (such as sample J4 in Electronic Appendix EA3) would have to assimilate (>60% metasediment) to reach the TiO_2 content of the target monzonitic magma (0.8 wt% TiO_2). This is, again, infeasible.

From the foregoing, it seems most probable that the crustal component evident in most of the Yzerfontein mafic to intermediate magmas was inherited mainly from enriched mantle with incorporation of a small component from the Malmesbury Group and Swartland complex metasediments.
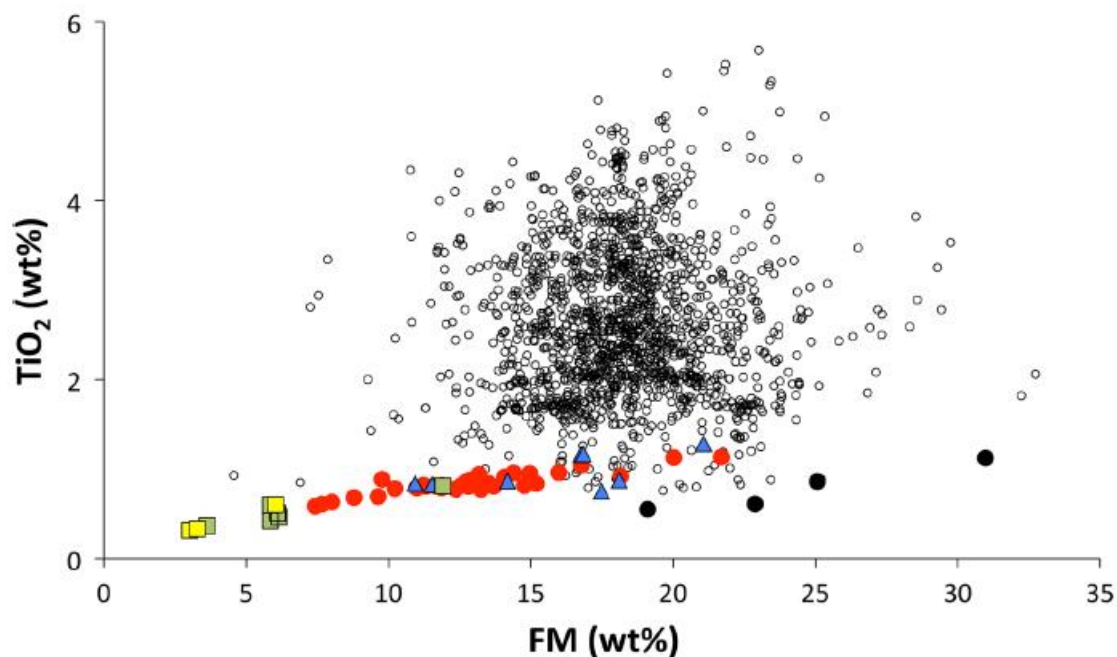
Fig. 14 Plot of TiO_2 against FM (FeO^T + MnO + MgO) for the Yzerfontein rocks (*symbols* as in Fig. 4) and 1601 alkali basalts (*small circles*). Data for the basalts were obtained from the EarthChem database (www. earthchem.org). See text for discussion

This metasedimentary component is necessary to account for the presence of inherited zircons in the Yzerfontein rocks and to satisfy the constraints from the Pb and Hf isotope data. Furthermore, since we are not dealing with bulk assimilation, the most credible assimilant would be small amounts of partial melt from the Malmesbury Group or Swartland complex. Significantly, such melts would probably carry disproportionately large amounts of zircon, liberated by biotite breakdown in melting reactions and selectively entrained into the melts (Stevens et al. 2007; Clemens and Stevens 2012).

As noted above, the most credible model for the proposed mantle enrichment involves subduction and possible reaction between slab-derived fluids and rocks of the ultramafic mantle wedge. In the region under consideration, Kisters et al. (2015) interpret the Malmesbury Group to be at least 25 km thick and assign to it a fore-arc setting, with around 30 Myr of subduction having occurred between 575 and 545 Ma. Such a period

of subduction could certainly have produced the inferred enriched character of the mantle wedge here, providing a suitable protolith for the shoshonitic magmas of the Yzerfontein pluton and imparting the 'primary' crustal signature evident in the chemistry and radiogenic isotope ratios for the rocks. The U–Pb and Hf isotope data on the inherited zircons in the Yzerfontein pluton suggest hybridisation with small volumes of felsic magmas formed from the Malmesbury Group or Swartland complex. We see no mixing trends between the CGS S-type magmas (inferred to be derived from the Malmesbury Group or Swartland complex) and the magmas of the Yzerfontein pluton, and a complete absence of Malmesbury Group or Swartland complex xenoliths in the Yzerfontein rocks. This observation is further evidence against bulk assimilation of the basement metasedimentary rocks. Being highly refractory, the selectively entrained zircon crystals would dominate the U–Pb and Hf isotope chemistry of the system, and the proportion of crustal assimilation would appear to be very much greater than it actually was. It is not possible to model these minor, selective assimilation processes because we have no statistically valid average for the proportion of inherited cores in Yzerfontein zircons or indeed information on the textural distribution of detrital zircons in the metasedimentary source rocks. Thus, we cannot legitimately infer the proportion of assimilated Malmesbury Group or Swartland complex from the zircon data.

Conclusions

The composite Yzerfontein pluton contains mainly mafic to intermediate rocks belonging to the shoshonitic series, together with some felsic differentiates and minor other magma groupings. It has now been dated to 535 Ma, contemporaneous with the voluminous late syn- to post-tec- tonic S- and I-type granitic magmatism of the Cape Granite Suite. The Yzerfontein parent magmas were most probably derived through partial melting of mantle that had been enriched by metasomatic fluids and perhaps by solids from an oceanic slab and its blanket of sedimentary material, up to 30 Myr before the mantle partial melting events. Evidence from the U–Pb ages and Hf isotope compositions of the zircons in the rocks suggests that the Yzerfontein shoshonitic magmas were also hybridised through small degrees of sub-emplacement-level interactions with the metasedimentary crust of the Malmesbury Group and Swartland complex. There is no apparent magmatic kinship between the Yzerfontein pluton and the I-type granitic rocks of the CGS. Although there is good evidence for mingling between mafic and intermediate magmas in the Yzerfontein pluton, the field, chemical and isotopic data suggest that this does not constitute magma mixing, and the igneous enclaves are mostly autoliths, rather than extraneous magmas. The chemical and isotopic characteristics, and lack of mixing trends among the Yzerfontein rocks, means that the mantle protolith was itself heterogeneous, containing rocks with varying degrees of crustal influence. Partial melting of large volumes of the middle to deep crust, to produce the CGS granitic magmas, required advection of significant mantle thermal energy into the deep crust. The most likely vector for this extracrustal heat would be mantle-derived magmas. Following the inferences of Kisters et al. (2015), this mantle event may have been triggered by either ridge subduction or, perhaps more likely, the opening of a slab window. It is, thus, possible that the mafic to intermediate rocks of the Yzerfontein pluton (and others like it in the region) represent a small fraction of this mafic heat source that was emplaced into the shallow crust. The implication of this is twofold. First, the deep crust in the region probably now contains a

large volume of gabbroic to dioritic rock and, second, that the rocks of the deep Malmesbury Group and Swartland complex would have reached the granulite facies of metamorphism at the time of generation and emplacement of the felsic plutonic and volcanic magmas of the CGS. This very late- to post-collisional magmatism probably represented the final stage in cratonisation of this part of southern Africa, but also represented significant crustal growth by underaccretion (e.g., Rudnick 1990).

References

Armstrong R, De Wit J, Reid D, York D, Zartman R (1998) Cape town's table mountain reveals rapid Pan-African uplift of its basement rocks. J African Earth Sci 27(1A):10–11

Belcher RW, Kisters A (2003) Lithostratigraphic correlations in the western branch of the Pan-African Saldania belt, South Africa: the Malmesbury Group revisited. S Afr J Geol 106(4):327–342. doi:10.2113/106.4.327

Bierlein FP, Arne DC, Keay SM, McNaughton NJ (2001) Timing relationships between felsic magmatism and mineralisation in the central Victorian gold province, southeast Australia. Aust J Earth Sci 48:883–899

Chemale EJ, Scheepers R, Gresse PG, van Schmus WR (2011) Geochronology and sources of late Neoproterozoic to Cambrian granites of the Saldania Belt. Int J Earth Sci 100:431–444. doi:10.1007/s00531-010-0579-1

Clemens JD (1990) The granulite – granite connexion. In: Vielzeuf D, Vidal P (eds) Granulites and crustal differentiation. Kluwer Academic Publishers, Dordrecht, pp 25–36

Clemens JD (2006) Melting of the continental crust: fluid regimes, melting reactions and source-rock fertility. In: Rushmer T, Brown M (eds) Evolution and differentiation of the continental crust. Cambridge University Press, Cambridge, pp 297–331

Clemens JD (2012) Granitic magmatism, from source to emplacement: a personal view. Appl Earth Sci 121(3):107–136. doi:10.1179/1 743275813Y.0000000023

Clemens JD, Phillips GN (2014) Inferring a deep-crustal source terrane from a high-level granitic pluton: the Strathbogie Batholith, Australia. Contrib Miner Petrol 168(5). doi:10.1007/ s00410-014-1070-y

Clemens JD, Stevens G (2012) What controls chemical variation in granitic magmas? Lithos 134–135:317–329. doi:10.1016/j. lithos.2012.01.001

Clemens JD, Stevens G (2016) The Saldanha Bay Caldera Complex: clarifying the Cambrian geology of the Postberg—Saldanha area of the West Coast, South Africa. S Afr J Geol 119(2):347– 358. doi:10.2113/gssajg.119.2.347

Clemens JD, Regmi K, Nicholls IA, Weinberg R, Maas R (2016) The Tynong pluton, its mafic synplutonic sheets and igneous microgranular enclaves: the nature of the mantle connection in I-type granitic magmas. Contrib. Mineral. Petrol. 171(4):1–17. doi:10.1007/s00410-016-1251-y

Clemens JD, Stevens G, Elburg MA (2017) Petrogenetic processes in granitic magmas and their igneous microgranular enclaves from Central Victoria, Australia: match or mismatch? Trans R Soc S Afr 72(1):6–32. doi:10.1080/0035919X.2016.1209702

Da Silva LC, Gresse PG, Scheepers R, McNaughton NJ, Hartmann LA, Fletcher I (2000) U–Pb SHRIMP and Sm-Nd age constraints on the timing and sources of the Pan-African Cape Granite Suite, South Africa. J Afr Earth Sci 30(4):795–815

Dorais M, Whitney JA, Roden MF (1990) Origin of mafic enclaves in the Dinkey Creek pluton, central Sierra Nevada Batholith, California. J Petrol 31:853–881. doi:10.1093/petrology/31.4.853

Dudás FÖ (2012) Geochemistry of igneous rocks from the Crazy Mountains, Montana, and tectonic models for the Montana Alkalic Province. J Geophys Res Solid Earth 96(B8):13261– 13277. doi:10.1029/91JB00246

Elburg MA, Nicholls IA (1995) Origin of microgranitoid enclaves in the S-type Wilsons Promontory batholith, Victoria—evidence for magma mingling. Aust J Earth Sci 42:423–435. doi:10.1080/08120099508728212

Enggist A, Luth RW (2016) Phase relations of phlogopite and pyroxene with magnesite from 4 to 8 GPa: KCMAS–H_2O and KCMAS–H_2O–CO_2. Contrib Miner Petrol 171:88. doi: 10.1007/s00410-016-1304-2

Frimmel HE, Basei MAS, Correa VX, Mbangula N (2013) A new lithostratigraphic subdivision and geodynamic model for the Pan-African western Saldania Belt, South Africa. Precambrian Res 231:218–235. doi:10.1016/j.precamres.2013.03.014

Glazner AF, Coleman DS, Mills RD (2015) The volcanic-plutonic connection. In: Breitkreuz C, Rocchi S (eds) Advances in volcanology. Springer, Berlin, pp 1–22

Goscombe BD, Gray DR (2008) Structure and strain variation at mid-crustal levels in a transpressional orogen: a review of the Kaoko Belt structure and the character of West Gondwana amalgamation and dispersal. Gondwana Res 13(1):45–85. doi:10.1016/j.gr.2007.07.002

Goscombe BD, Hand M, Gray D (2003) Structure of the Kaoko Belt, Namibia: progressive evolution of a classic transpressional orogen. J Struct Geol 25(7):1049–1081. doi:10.1016/ S0191-8141(02)00150-5

Gresse PG, von Veh MW, Frimmel HE (2006) Namibian (Neoproterozoic) to early Cambrian Successions. In: Johnson MR, Anhaeusser CR, Thomas RJ (eds) The geology of South Africa, vol. Geological Society of South Africa/Council for Geoscience, Johannesburg/Pretoria, pp 395–420

Griffin WL, Wang X, Jackson SE, Pearson NJ, O'Reilly SY, Xu X, Zhou X (2002) Zircon chemistry and magma mixing, SE China: in situ analysis of Hf isotopes.Tonglu and Pingtan igneous complexes. Lithos 61(3–4):237–269. doi:10.1016/ S0024-4937(02)00082-8

Harris C, Vogeli J (2010) Oxygen isotope composition of garnet in the Peninsula granite, Cape Granite Suite, South Africa: constraints on melting and emplacement mechanisms. S Afr J Geol 113(4):401–412. doi:10.2113/gssajg.113.4.401

Hartnady CJH, Newton AR, Theron JN (1974) The stratigraphy and structure of the Malmesbury Group in the southwestern Cape. Bull Univ Cape Town Precam Res Unit 15:193–213

Hugo D (2011) Petrological investigation of the Yzerfontein layered mafic complex, West Coast, South Africa. BSc (Hons) thesis (unpubl.), Department of Earth Sciences, University of Stellenbosch

Jordaan LJ (1990) The geology and geochemistry of mafic and intermediate igneous rocks associated with the Cape granites. MSc thesis (unpubl.), Department of Geology, University of Stellenbosch, p 243

Jordaan LJ, Scheepers R, Barton ES (1995) The geochemistry and isotopic composition of the mafic and intermediate components of the Cape Granite Suite, South Africa. J Afr Earth Sci 21(1):59– 70. doi:10.1016/0899-5362(95)00075-5

Kisters AFM, Belcher RW (2017) The stratigraphy and structure of the western Saldania Belt, South Africa. In: Basei M, Oyhantcabal P, Siegesmund S (eds) Geology of SW Gondwana. Springer, New York **(in press)**

Kisters AFM, Belcher RW, Armstrong RA, Scheepers R, Rozendaal A, Jordaan LS (2002) Timing and kinematics of the Colenso Fault; The Early Paleozoic shift from collisional to extensional tectonics in the Pan-African Saldania Belt, South Africa. S Afr J Geol 105(3):257–270. doi:10.2113/1050257

Kisters AFM, Agenbach C, Frei D (2015) Age and tectonic significance of the volcanic Bloubergstrand member in the Pan-african Saldania Belt, South Africa. S Afr J Geol 18(3):213–224. doi:10.2113/gssajg.118.3.213

Le Bas MJ, Streckeisen AL (1991) The IUGS systematics of igneous rocks. J Geol Soc Lond 148:825–833

Le Maitre RW, Streckeisen A, Zanettin B, Le Bas MJ, Bonin B, Bateman P, Belleni G, Dudek A, Efremova S, Keller J, Lamere J, Sabine PA, Schmid R, Sorensen H, Wolley AR (2002) Igneous rocks: a classification and glossary of terms, recommendations of the international union of geological sciences, subcommission of the systematics of igneous rocks. Cambridge University Press, Cambridge

Maske S (1957) The diorites of Yzerfontein, Darling, Cape Province. Annals Univ. Stellenbosch 33(Section A, 1-11): 3–68

Middlemost EAK (1994) Naming materials in the magma igneous rock system. Earth-Sci Rev 37(3–4):215–224. doi:10.1016/0012-8252(94)90029-9

Pearce JA, Cann JR (1973) Tectonic setting of basic volcanic rocks determined using trace element analyses. Earth Planet Sci Lett 19(2):290–300. doi:10.1016/0012-821X(73)90129-5

Pin C (1990) Evolution of the lower crust in the Ivrea Zone: a model based on isotopic and geochemical data. In: Vielzeuf D, Vidal P (eds) Granulites and crustal evolution. Kluwer Academic Publishers, Dordrecht, pp 87–110

Pitcher WS (1997) The nature and origin of granite. Chapman & Hall, London, p 387

Rosenbaum G, Li P, Rubatto D (2012) The contorted New England Orogen (eastern Australia): New evidence from U–Pb geochronology of early Permian granitoids. Tectonics 31: TC1006, doi: 10.1029/2011TC002960

Rotenberg E, Davis DW, Amelin Y, Ghosh S, Bergquist BA (2012) Determination of the decay constant of ^{87}Rb by laboratory accumulation of ^{87}Sr. Geochim Cosmochim Acta 85:41–57

Rudnick R (1990) Continental crust—growing from below. Nature 347:711–712

SACS (South African Committee for Stratigraphy) (1980) Stratigraphy of South Africa. Part 1. In: Kent LE (ed) Lithostratigraphy of the Republic of South Africa, SW Africa/Namibia, and the Republics of Bophuthatswana, Transkei and Venda, vol 8. Handbook of the Geological Survey of South Africa

Sambridge MS, Compston W (1994) Mixture modelling of multi-component data sets with application to ionprobe zircon ages. Earth Planet Sci Lett 128(3):373–390. doi:10.1016/0012-821X(94)90157-0

Scheepers R (1995) Geology, geochemistry and petrogenesis of Late Precambrian S-, I- and A-type granitoids in the Saldania belt, Western Cape Province South Africa. J Afr Earth Sci 21:35–58. doi:10.1016/0899-5362(95)00087-A

Scheepers R, Armstrong R (2002) New U–Pb SHRIMP zircon ages of the Cape Granite Suite: implications for the magmatic evolution of the Saldania Belt. S Afr J Geol 105(3):241–256. doi:10.2113/1050241

Scheepers R, Nortjé AN (2000) Rhyolitic ignimbrites of the Cape Granite suite, southwestern Cape province, South Africa. J Afr Earth Sc 31(3):647–656

Scheepers R, Poujol M (2002) U–Pb zircon age of Cape Granite Suite ignimbrites: characteristics of the last phases of the Saldanian magmatism. S Afr J Geol 105(2):163–178. doi:10.2113/105.2.163 Scheepers R, Schoch AE (2006) The Cape Granite Suite. In: Johnson MR, Anhaeusser CR, Thomas RJ (eds) The geology of South Africa, vol. Geological Society of South Africa/Council for Geoscience, Johannesburg/Pretoria, pp 421–432

Słaby E, Martin H (2008) Mafic and felsic magma interaction in granites: the Hercynian Karkonosze pluton (Sudetes, Bohemian Massif). J Petrol 49(2):353–391. doi:10.1093/petrology/egm085

Stevens G, Villaros A, Moyen J-F (2007) Selective peritectic garnet entrainment as the origin of geochemical diversity in S-type granites. Geology 35(1):9–12. doi:10.1130/g22959a.1

Thompson AB (1990) Heat, fluids and melting in the granulite facies. In: Vielzeuf D, Vidal P (eds) Granulites and crustal differentiation. Kluwer Academic Publishers, Dordrecht, pp 37–58

Vernon RH (1984) Microgranitoid enclaves in granites—globules of hybrid magma quenched in a plutonic environment. Nature 309:438–439

Vielzeuf D, Clemens JD, Pin C, Moinet E (1990) Granites, granulites and crustal differentiation. In: Vielzeuf D, Vidal P (eds) granulites and crustal differentiation. Kluwer Academic Publishers, Dordrecht, pp 59–86

Villaros A (2010) Petrogenesis of S-type Granite with Particular Emphasis on Source Processes: The Example of the S-type Granite of the Cape Granite Suite. PhD thesis (unpubl.), Department of Earth Sciences, University of Stellenbosch, Stellenbosch, p 225

Villaros A, Stevens G, Buick IS (2009) Tracking S-type granite from source to emplacement: clues from garnet in the Cape Granite Suite. Lithos 112(3–4):217–235. doi:10.1016/j.lithos.2009.02.011 Villaros A, Buick IS, Stevens G (2012) Isotopic variations in S-type granites: an inheritance from a heterogeneous source? Contrib Miner Petrol 163(2):243–257. doi:10.1007/s00410-011-0673-9

Wedepohl KH (1995) The composition of the continental crust. Geochim Cosmochim Acta 59(7):1217–1239. doi:10.1016/0016-7037(95)00038-2

White AJR, Chappell BW (1977) Ultrametamorphism and granitoid genesis. Tectonophysics 43:7–22

Wyllie PJ, Sekine T (1982) The formation of mantle phlogopite in subduction zone hybridization. Contrib Miner Petrol 79(4):375–380. doi:10.1007/BF01132067